

# The spectrum of a Gross-Neveu Yukawa model with flavor disorder in $d = 3$

Shiroman Prakash

*Department of Physics and Computer Science,  
Dayalbagh Educational Institute, Agra 282005, India  
E-mail: sprakash@dei.ac.in*

## Abstract

We study a variant of the Gross-Neveu-Yukawa model, containing  $M$  real scalar fields and  $N$  Dirac (or Majorana) fermions, interacting via a Yukawa interaction with a local Gaussian random coupling in three dimensions. In the limit where  $M$  and  $N$  are both large, and the ratio  $M/N$  is held fixed, the model defines a line of infrared fixed points parameterized by  $M/N$ , reducing to the familiar large  $N$  Gross-Neveu vector model when  $M/N = 0$ . When  $M/N$  is non-zero, the model is dominated by melonic diagrams and gives rise to SYK-like physics. We compute the spectrum of single-trace operators in the theory, and find that it is real for all values of  $M/N$ . We conclude that the model provides a real non-supersymmetric generalization of the SYK model to three-dimensions.

# 1 Introduction

The large- $N$  limit [1] is a powerful tool to understand strongly-interacting quantum field theories. In this limit, fluctuations are suppressed, and unexpected, classical descriptions can emerge – the most notable example of which is classical gravity in anti-de Sitter space [2–4] for certain conformal field theories.

Originally, two large  $N$  limits were known to exist – the large  $N$  limit of theories with dynamical fields in the adjoint representation, exemplified by [1], in which all planar Feynman diagrams contribute, and theories whose dynamical fields are in the vector representation, exemplified by [5], in which only a small summable subset of planar Feynman diagrams contribute. Large  $N$  vector models typically possess a slightly broken higher-spin symmetry, and any dual gravitational description for such a large  $N$  CFT would involve a tower of massless higher-spin gauge fields [6–12]. On the other hand, strongly-interacting large  $N$  adjoint/matrix models are, at least in some cases with sufficient supersymmetry [2, 13], known to be dual to theories of traditional Einstein supergravity.

There also exist theories whose large  $N$  limit interpolates between a vector model and an adjoint/matrix model. The ABJ theory [14] is a bifundamental  $U(N) \times U(M)$  Chern-Simons theory that can be studied in the limit where  $M$  and  $N$  are both large and the ratio  $M/N$  is held fixed. When  $M/N \ll 1$ , the theory possesses a slightly-broken higher-spin symmetry and is effectively a vector model, dual to a higher-spin gauge theory with  $U(N)$  Chan Paton indices for the higher-spin gauge fields [15]. When  $M/N = 1$ , the theory becomes ABJM theory [13] and is dual to type IIA supergravity in  $AdS_4 \times CP_3$  at strong coupling. The parameter  $M/N$  can be understood as a gravitational 't Hooft coupling in the bulk; as this parameter is increased from zero to one, the higher spin gage fields somehow coalesce to form strings.

Large  $N$  vector model CFT's without supersymmetry are common. Do there exist large  $N$  CFT's without supersymmetry that could be dual to non-supersymmetric theories of Einstein gravity in AdS? A variant of the weak gravity conjecture [16] suggests that the answer to this question is no<sup>1</sup>. However, motivated by the example of ABJ [15], one may try to promote non-supersymmetric vector models to bifundamental theories, and study their behaviour as a function of  $M/N$ , as discussed in [17]. All examples studied so far become complex at some critical finite value of  $M/N$ , as can be seen via the epsilon expansion, as discussed in [17, 18], in accordance with expectations from the conjecture of [16], or, in the case of certain Chern-Simons theories with matter [19, 20], cannot be studied at strong coupling.

More recently, a third large  $N$  limit – the melonic limit<sup>2</sup> – has come into attention, via the study of the Sachdev-Ye Kitaev (SYK) model [31–35]. The SYK model is tractable chaotic model in one dimension, exhibiting features of black hole physics, and has attracted considerable attention in the literature, e.g., [36–42]. The melonic limit is dominated by a subset of planar diagrams that is explicitly summable yet still manages to capture non-trivial aspects of gravitational physics.

Does there exist a natural non-supersymmetric higher-dimensional generalization of the SYK model [43–47]? While supersymmetric generalizations exist, all non-supersymmetric constructions, [44, 45, 47] encounter the problem of an operator with a complex scaling dimension. Similar results have also been observed in tensor models, e.g., [29, 48–50]. In particular, [47] defined a “biconical” SYK model that depends on  $M$  and  $N$ , that interpolates between the critical  $O(N)$  vector model when  $M/N \ll 1$  and a model with SYK like physics when  $M/N$  is finite, much like ABJ. They

---

<sup>1</sup>However, we remark that a precise statement of the implications of various weak gravity and swampland conjectures related to [16] for the existence of strongly interacting large  $N$  CFTs without supersymmetry may still be lacking.

<sup>2</sup>The melonic limit was first understood in the context of tensor models. See e.g., [21–30]

found the model becomes complex when  $M/N$  exceeds 0.22, much like bifundamental models of critical scalars in  $d = 3$  [17, 18]. By contrast, [47] shows that supersymmetric version of the theory is real for all values of  $M/N$ .

It is natural to expect that non-supersymmetric melonic CFT's do not exist – and, if this expectation is true, it would provide strong support for the conjecture that non-supersymmetric strongly interacting CFT's dominated by planar diagrams do not exist. In this paper, we will show that this expectation is false by computing the spectrum a simple example of a non-supersymmetric CFT, recently proposed in [51], dominated by melonic diagrams that can be studied for all values of  $M/N$ .

## 2 Gross-Neveu-Yukawa model with disorder

A natural starting point for a search for higher-dimensional SYK physics is the well-known Gross-Neveu (GN) model [52], which is asymptotically free in  $d = 2$ , and possesses a non-trivial ultraviolet fixed point in  $d = 2 + \epsilon$ , that, at least when  $N$  is large, defines a conformal field theory in  $d = 3$ . A tensorial generalization of the GN model was constructed in [49, 53, 54], but its spectrum of operators includes a complex mode – an identical spectrum would arise in a GN model with a random 4-fermion interaction. However, there exists a cousin of the Gross-Neveu model, known as the Gross-Neveu-Yukawa (GNY) model [55–58], that gives rise to an *infrared* fixed point in  $d = 4 - \epsilon$ , which is equivalent to the GN UV fixed point in  $d = 3$ , at least when  $N$  is sufficiently large, as reviewed in [57, 58]. See also, e.g., [59–75] and references therein.

Inspired by [47], we study a variant of the Gross-Neveu Yukawa model constructed by [51]. The model is closely related to several one-dimensional generalizations of the SYK model [76–81], and, as discussed in [51], several lattice realizations on a honeycomb lattice exist for the  $d = 3$  model.

The model of [51] consists of  $M$  real scalar fields,  $\sigma^a$ ,  $a = 1, \dots, M$ , and  $N$  Dirac or Majorana fermions,  $\psi^i$ ,  $i = 1, \dots, N$  with the following interaction,

$$\mathcal{S}_{int} = \int d^d x g_{ai}{}^j \sigma^a \bar{\psi}^i \psi_j. \quad (2.1)$$

If  $\sigma$  is dynamical, the above interaction is relevant for  $d < 4$ , and may lead to interacting IR fixed point in  $d = 3$ .<sup>3</sup> If  $\sigma$  is non-dynamical, the above interaction is irrelevant for  $d > 2$  – but, when  $N$  is large, could define an interacting UV fixed point in  $d = 3$ , similar to the GN fixed point in  $d = 3$ .

We take  $g_{ai}{}^j$  to be a random coupling with quenched disorder, with zero mean  $\langle g_{ai}{}^j \rangle = 0$ , but non-zero variance

$$\langle g_{ai}{}^j g_{bk}{}^l \rangle = \frac{J}{N^2} \delta_{ab} \delta_i^l \delta_k^j, \quad (2.2)$$

parameterized by the dimensionful constant  $J$ . We emphasize the theory contains flavour disorder and not spatial disorder which is present in the related model of [82, 83]. The resulting average is invariant under  $O(M) \times U(N)$  for the theory with Dirac Fermions or  $O(M) \times O(N)$  for the theory with Majorana fermions. The theory with Dirac fermions possesses a global  $U(1)$  symmetry<sup>4</sup> and

<sup>3</sup>There is also a classically relevant term  $\sigma^4$ . In the melonic limit, the  $\sigma^4$  generated from the Yukawa coupling is suppressed by  $1/N$ , and we assume it can be tuned to zero. A disordered  $g_{abcd}^{(2)} \sigma_a \sigma_b \sigma_c \sigma_d$  coupling, with zero mean but non-zero variance, is irrelevant for small  $M/N$ , but may be relevant above critical value of  $M/N = \frac{11}{4} (\sqrt{2} - 1)$ , possibly leading to a new melonic fixed point that we do not investigate in the present work.

<sup>4</sup>In 2-dimensional supersymmetric SYK models, the presence of a global symmetry is associated with a “double zero” of the integration kernel equation  $k(\tau) - 1 = 0$ , leading to problems as described in [44]. We do not seem to see this effect in our model in  $d = 3$ .

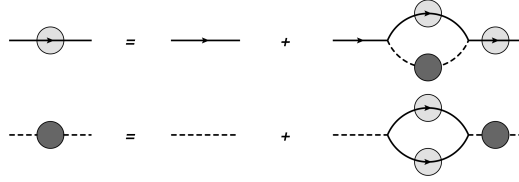


Figure 1: The gap equations for the exact propagators  $G(p)$  and  $F(p)$ . Dashed lines denote scalar propagators and solid lines denote fermion propagators.

contains both even and odd spin single-trace operators; while the theory with Majorana fermions has no global  $U(1)$  symmetry and contains only even spin single-trace operators.

We take both  $M$  and  $N$  to be large, and keep the ratio  $\lambda = \frac{M}{N}$  held fixed. In this limit, it follows from the analysis in [84] that this theory is dominated by melonic diagrams.

When  $M = 1$ , one can eliminate the random coupling via field redefinition, and the theory reduces to the GN model when  $\lambda = 0$ . However, corrections in  $\lambda = M/N$  to the disordered theory in our limit are not the same as  $1/N$  corrections to the GN/GNY models—only melonic diagrams contribute to  $\frac{M}{N}$  corrections to the disordered GNY model, while non-melonic diagrams contribute to  $1/N$  corrections to the GN model.

[51] studied the scrambling in the above model in  $d = 2$ , however, the existence of a CFT with real spectrum in  $d = 3$  was not established. Here, we compute the spectrum of single-trace operators in  $d = 3$  to answer whether or not the model defines a real unitary conformal field theory in  $d = 3$ , or, if, like all other known non-supersymmetric SYK models in higher dimensions, the spectrum included an operator with complex scaling dimension for  $M/N$  sufficiently large. We find the spectrum of single-trace operators in  $d = 3$  is real for all values of  $M/N$ .

We present the spectrum for the  $N$  Dirac fermions below – the spectrum of the theory with  $2N$  Majorana fermions is a truncation of this spectrum to operators with even spin.

### 3 Exact propagators

Before we compute the spectrum, we need the exact propagators in the theory for  $\psi$  and  $\sigma$ . These were obtained earlier in [51] as we review below.

Denote the exact propagator for the  $\sigma$  field by  $F(p)$ , and the exact propagator for the fermionic field by  $G(p)$ :

$$\langle \psi^i(p) \bar{\psi}_j(-q) \rangle = (2\pi)^d G(p) \delta^d(p - q) \delta_j^i, \quad \langle \sigma^a(p) \sigma^b(-q) \rangle = (2\pi)^d G(p) \delta^d(p - q) \delta^{ab}. \quad (3.1)$$

$G(p)$  is a matrix in spinor-space. We work in  $d$ -dimensions, and take the dimension of  $\gamma$ -matrices to be a free parameter  $d_\gamma$ .

In the melonic limit, the exact propagators satisfy the gap equations shown in Figure 1. These equations can be written as

$$F_0(p)^{-1} = F(p)^{-1} - J \int \frac{d^d q}{(2\pi)^d} \text{tr} (G(q) G(p + q)) \quad (3.2)$$

$$G_0(p)^{-1} = G(p)^{-1} + J\lambda \left( \int \frac{d^d q}{(2\pi)^d} G(p - q) F(q) \right). \quad (3.3)$$

where  $G_0(p) = \frac{1}{i\not{p}}$  and  $F_0(p) = \frac{1}{p^2}$  are free propagators.

We search for an infrared solution to these equations. Our conformal ansatz for interacting propagators is

$$G(p) = A \frac{i\psi}{p^{2a+1}}, \quad F(p) = \frac{B}{p^{2b}}. \quad (3.4)$$

The scaling dimensions of  $\psi$  and  $\sigma$  in position space are related to  $a$  and  $b$  via  $\Delta_\psi = (d - 2a)/2$  and  $\Delta_\sigma = (d - 2b)/2$ .

We require  $a < 1/2$  to drop the free propagator<sup>5</sup>  $G_0(p)$  in comparison to  $G(p)$  in the infrared. We also require  $b < 1$  to drop  $F_0(p)$  in comparison to  $F(p)$ . When we drop the  $F_0(p)$  term, we obtain the relation

$$2b = d - 4a, \text{ or, } 2\Delta_\psi + \Delta_\sigma = d. \quad (3.5)$$

The allowed range for  $a$  then becomes

$$(d - 2)/4 < a < 1/2. \quad (3.6)$$

Evaluating equations (3.2) and (3.3) using the conformal ansatz, we obtain,

$$\lambda = \frac{\sqrt{\pi} d_\gamma 2^{2a-d+2} \cos(\pi a) \csc(2\pi a - \frac{\pi d}{2}) \Gamma(a + \frac{d}{2} + \frac{1}{2})}{(4a - d)\Gamma(2a)\Gamma(\frac{d}{2} - a)}, \quad (3.7)$$

which determines the allowed scaling dimension of the fermion in the infrared limit. In terms of  $\Delta_\psi$ , in  $d = 3$ , the equation becomes

$$\lambda = \frac{8(2\Delta_\psi - 5)(2\Delta_\psi - 3) \sin^3(\pi\Delta_\psi) \cos(\pi\Delta_\psi) \Gamma(3 - 4\Delta_\psi) \Gamma(4\Delta_\psi - 4)}{\pi}. \quad (3.8)$$

As shown in Figure 2, in  $d = 3$  there is a unique solution for  $\Delta_\psi$  in the allowed range, for any value of  $\lambda$ .

For small  $\lambda$ , in  $d = 3$ , the solution to the gap equation is:

$$\Delta_\psi = 1 + \frac{2\lambda}{3\pi^2} + \frac{80\lambda^2}{27\pi^4} - \frac{(120\pi^2 - 4384)\lambda^3}{243\pi^6} + O(\lambda^4). \quad (3.9)$$

This agrees with the  $O(1/N)$  expression of the anomalous dimension of  $\psi$  in the Gross-Neveu model but not the  $O(1/N^2)$  expression, as expected because  $M^2/N^2$  differs from  $1/N^2$  at the level of Feynman diagrams.

When  $\lambda = 1$ , we find, numerically, that  $\Delta_\psi = 1.10746$  and  $\Delta_\sigma = 0.785078$ . As  $\lambda \rightarrow \infty$ ,  $\Delta_\psi \rightarrow 5/4$  and  $\Delta_\sigma \rightarrow 1/2$ . In between, there is a ‘‘critical value’’ of  $\lambda_* = \frac{2(d-1)d_\gamma}{d+2} = \frac{8}{5}$  defined by the condition  $2\Delta_\sigma = 2\Delta_\psi - 1$ , as discussed below, for which  $\Delta_\sigma = 2/3$  and  $\Delta_\psi = 7/6$ .

Does the free solution flow to the putative IR limit identified above? In Appendix A, we solve the gap equations (3.2) and (3.3) from UV to IR, for the extreme values of  $\lambda$ ,  $\lambda = 0$  (analytically) and  $\lambda = \infty$  (numerically), that interpolate between the free propagators in the UV and the interacting propagators in the IR. We expect that similar flows also exist for intermediate values of  $\lambda$ .

## 4 Operator spectrum

We now compute the single-trace operator spectrum. These are bilinears which are singlets under the  $O(M) \times U(N)$  symmetry group.<sup>6</sup> The single-trace operators contained in the free theory are

<sup>5</sup>When dropping the free propagator  $F_0$  and  $G_0$ , it may appear as if the kinetic terms are playing no role in the theory and  $e^{i\alpha(x)}\psi(x)$  would have exactly the same action as  $\psi(x)$ . However, as discussed in [44], in higher-dimensions such zero-modes are expected to be non-normalizable and therefore do not lead to a divergence.

<sup>6</sup>Note that bilinears such as  $\sigma_a \psi_i$  or, more generally  $\sigma_a A^{ai} \psi_i$ , for any  $M \times N$  complex matrix  $A$ , are not invariant under the  $O(M) \times U(N)$  symmetry group. In the melonic limit, anomalous dimensions of such operators are suppressed

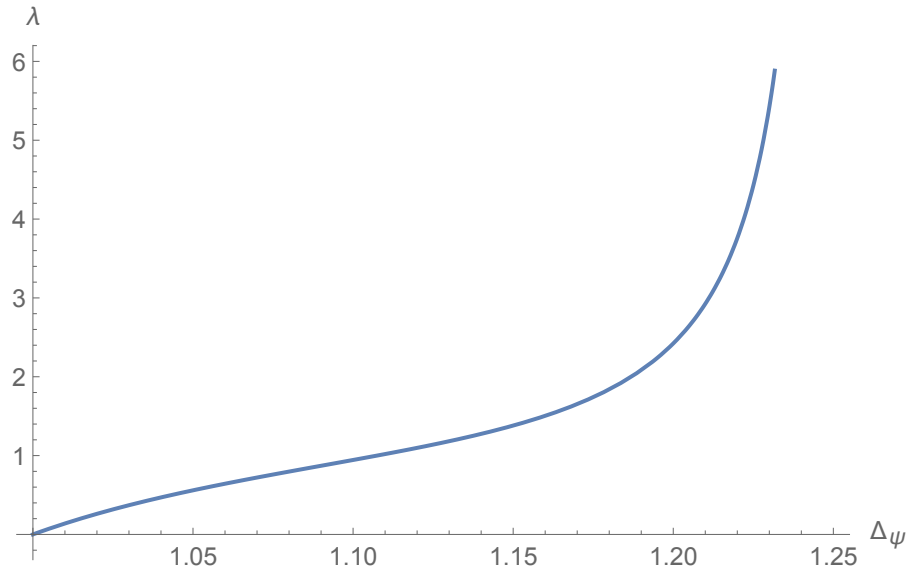


Figure 2: The gap equation for  $\Delta_\psi$  in  $d = 3$ . We see that there is a unique solution for any value of  $\lambda$ .

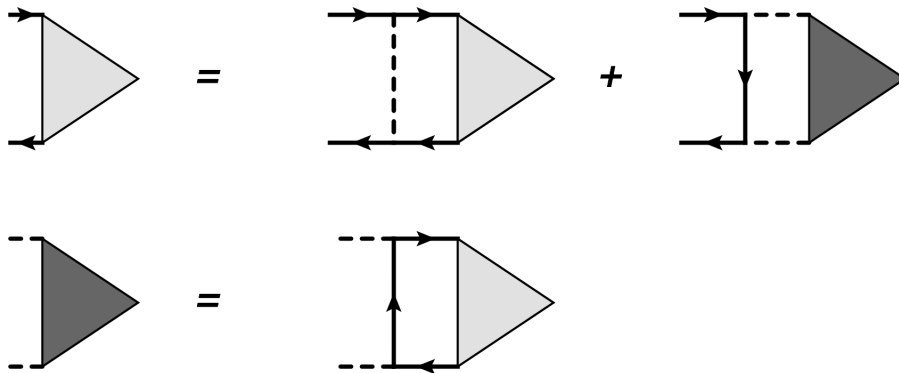


Figure 3: In the melonic IR limit, the exact three-point functions  $\langle \sigma(x_1)\sigma(x_2)\mathcal{O}_{\tau,s}(x_3) \rangle$  and  $\langle \psi(x_1)\bar{\psi}(x_2)\mathcal{O}_{\tau,s}(x_3) \rangle$  (depicted as a dark and light grey triangle respectively) satisfy the ladder equation depicted. All propagators are exact propagators.

1. spin- $s$  bilinears of  $\psi$ , which are of the schematic form, for  $s = 0$ ,

$$\mathcal{A}_{0,n} \sim \bar{\psi}^i (\partial \cdot \gamma)^n \psi_i,$$

and, for  $s > 0$ ,  $\mathcal{A}_{s,n} \sim \bar{\psi}^i \gamma \cdot z (\partial \cdot z)^{s-1} (\partial \cdot \gamma)^n \psi_i$ , and

2. spin- $s$  bilinears of  $\sigma$ , which only exist for even spin  $s$ , and are of the schematic form

$$\mathcal{B}_{s,2m} \sim \sigma^a (\partial \cdot z)^s (\partial^{2m}) \sigma^a.$$

Here,  $z$  denotes a null polarization vector satisfying  $z^2 = 0$ , as in, e.g., [85, 86]. If  $\psi$  is a Majorana fermion, the fermion bilinears with odd-spin vanish identically.

In the interacting theory, some of these operators can mix depending on their parity. First consider the scalar operators. In  $d = 3$ , recall that  $\bar{\psi}\psi$  is a parity-odd pseudo-scalar, while  $\sigma^2$  is a parity-even scalar. Therefore,  $\mathcal{A}_{0,n}$  is parity-odd when  $n$  is even, and parity-even when  $n$  is odd.  $\mathcal{B}_{0,2m}$  is parity-even, and can mix with  $\mathcal{A}_{0,n}$  only when  $n$  is odd.

Let us now consider operators of nonzero spin. The operator  $\mathcal{B}_{s,2m}$  is parity even and only exists for even  $s$ . For even  $s$ , the operator  $\mathcal{A}_{s,n}$  is parity-even only when  $n$  is even, in which case it can mix with  $\mathcal{B}_{s,2m}$ . When  $n$  is odd,  $\mathcal{A}_{s,n}$  is parity-odd and cannot mix with scalar bilinears.

Denote the mixtures of fermion and scalar bilinears with well defined scaling dimensions as  $\mathcal{O}_{s,\tau}$  where  $\tau = \Delta_{\mathcal{O}} - s$ . In the IR limit, the conformally invariant three-point functions  $\langle \sigma(x_1) \sigma(x_2) \mathcal{O}_{\tau,s}(x_3) \rangle$  and  $\langle \psi(x_1) \bar{\psi}(x_2) \mathcal{O}_{\tau,s}(x_3) \rangle$  must satisfy the melonic ladder equation, shown schematically in Figure 3. We use this equation to determine the allowed operator-spectrum in the IR fixed point. This calculation is essentially the calculation of [87], and is sufficient to determine the spectrum in the SYK model, and its higher-dimensional bosonic generalizations. However, the computation is complicated slightly because of the existence of multiple allowed conformally-invariant forms for the three-point functions involving fermions [88, 85]. Details are presented in Appendix B.

## 5 Spectrum in $d = 3$

We present the spectrum of single-trace operators in the theory in  $d = 3$ , and observe that the spectrum is real for all  $\lambda$ . We focus on parity-odd and parity-even scalars, and leading-twist higher-spin operators (which are parity-even). We discuss the higher-twist parity-even and parity-odd higher-spin spectrum in Appendix C. We also briefly discuss the spectrum in  $d = 1$  and  $d = 4 - \epsilon$ , where analytic expressions can be obtained, in Appendix D.

### 5.1 Parity-Odd Scalars

In melonic models with a complex spectrum, such as [29, 48–50, 45, 47], the lowest-twist scalar typically has a complex scaling dimension. In our theory, this would be the lowest-twist parity-odd scalar, corresponding in the free theory to  $\bar{\psi}\psi$ . Let us, therefore, first compute the spectrum of parity-odd single-trace scalars.

We denote the scaling dimensions of parity-odd single-trace operators as  $\tilde{\Delta}_n$ , which we expect to take the form  $\tilde{\Delta}_n = 2\Delta_\psi + 2n + \tilde{\gamma}_{0,n}$ , with  $\tilde{\gamma}_{0,n} \rightarrow 0$  as  $n \rightarrow \infty$ .

From equation (B.23), we must solve,

$$K_0^{\text{odd}}(\tilde{\Delta}) = 1. \tag{5.1}$$

---

by  $1/N$ . One could also consider a different theory with  $O(N)$  symmetry group, based on real scalars and Majorana fermions, where such operators would be present, but we do not consider such a theory in the present work.

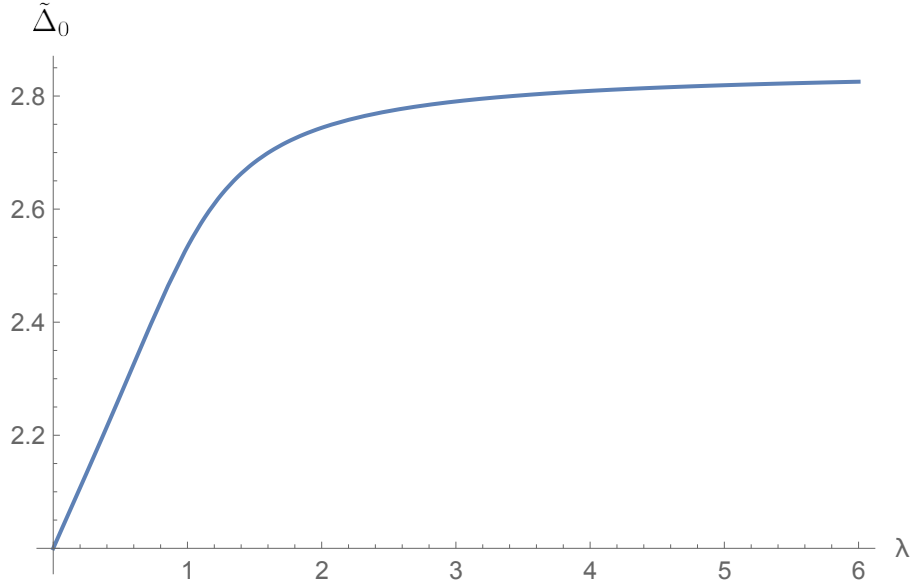


Figure 4: Scaling dimension of the lowest-twist parity-odd scalar,  $\bar{\psi}\psi$ , as a function of  $\lambda$ . The scaling dimension is real for all  $\lambda$ . (However, when  $\lambda = 0$ , the lowest-twist parity-odd scalar vanishes, and is not part of the spectrum.)

We solve this equation numerically, as illustrated in Appendix B.3. For  $\lambda = 1$ , we find the spectrum:  $\tilde{\Delta}_n = 2.53354, 4.25934, 6.23292, 8.22512, 10.2217, \dots$ , which approach  $2\Delta_\psi + 2n = 2.21492 + 2n$  as expected. For  $\lambda = \infty$ , we find the spectrum:  $\tilde{\Delta}_n = 2.85171, 4.66395, 6.60305, 8.57464, 10.5584, \dots$ , which approach  $2\Delta_\psi + 2n = 2.5 + 2n$  as expected. The behaviour for intermediate values of  $\lambda$  is similar, and, in fact, the spectrum is **real** for all values of  $\lambda$ . The scaling dimension of the lowest twist parity-odd scalar is shown as a function of  $\lambda$  in Figure 4.

For small  $\lambda$ , we find that,

$$\tilde{\Delta}_0 = 2 + \frac{16}{3\pi^2}\lambda - \frac{128}{27\pi^4}\lambda^2 + O(\lambda^3) = 2\Delta_\psi + \frac{4\lambda}{\pi^2} + O(\lambda^2). \quad (5.2)$$

The scaling dimensions for  $n \geq 1$  receive corrections that begin at order  $\lambda^2$ .

$$\begin{aligned} \tilde{\Delta}_n = 2\Delta_\psi + 2n + \frac{16}{3\pi^4 n(2n+1)}\lambda^2 + \\ \left( \frac{192(\log 2n + \gamma + 2) + 32}{27\pi^6 n^2} + O\left(\frac{1}{n^3}\right) \right) \lambda^3 + O(\lambda^4) \end{aligned} \quad (5.3)$$

At large  $n$ , we determined that

$$\tilde{\gamma}_{0,n} \sim \frac{1}{n^{2\Delta_\sigma}}, \quad (5.4)$$

which is consistent with the  $O(\lambda^3)$  expression in equation (5.3).

Let address a potential concern regarding the spectrum. When  $\lambda = 0$  the disordered spectrum is that of the large  $N$  GN model. One might also expect that the  $O(\lambda^1)$  correction to disordered spectrum matches the  $O(1/N)$  correction to the spectrum of the GN model, but this is not quite true. The  $1/N$  contribution to scaling dimension of the single-trace scalar primary in the GN model



is  $\tilde{\Delta}'_0 = 1 - \frac{16}{3\pi^2} \frac{1}{N}$ , which is the shadow of the value quoted for  $\tilde{\Delta}_0$  above when  $\lambda$  is replaced by  $1/N$ . The reason for this discrepancy is as follows. When  $M = 1$ , in the GN model, the scalar field  $\sigma$  can be integrated out, and its equation of motion sets  $\bar{\psi}\psi = 0$ , effectively replacing the scalar primary with  $\sigma$ . When one computes the  $1/N$  anomalous dimension of  $\sigma$  in the GN model, using e.g., Feynman diagrams, one obtains the correction  $-\frac{16}{3\pi^2} \frac{1}{N}$ , leading to the value  $\Delta'_0$  quoted above. However, in the disordered theory with  $M > 1$ , we cannot integrate out  $\sigma$ , so we cannot set  $\bar{\psi}\psi$  to zero – its scaling dimension becomes meaningful, and is equal to  $\tilde{\Delta}_0$  computed above for any  $\lambda > 0$ . The order  $\lambda$  correction to the scaling dimension of  $\sigma^a$  also does not match the  $1/N$  correction to the scaling dimension of  $\sigma$  in the GN model – this is because the Feynman diagrams that contribute to the  $1/N$  anomalous dimension of  $\sigma$  in the GN model include a non-melonic diagram that is suppressed by  $1/N$  rather than  $M/N$  in the disordered theory.

## 5.2 Parity-Even Scalars

We now compute the spectrum of parity-even scalars, which are mixtures of fermion and scalar bilinears. We find the spectrum includes operators (denoted as type A) whose scaling dimensions are of the form  $\Delta_n^A = 2\Delta_\psi + 2n + 1 + \gamma_{0,n}^A$  and operators (denoted as type B) whose scaling dimensions are of the form  $\Delta_n^B = 2\Delta_\sigma + 2n + \gamma_{0,n}^B$ , for  $n \geq 0$ , with  $\gamma_{0,n}^A, \gamma_{0,n}^B \rightarrow 0$  as  $n \rightarrow \infty$ .

Due to mixing, the integration kernel for parity-even scalars is a  $2 \times 2$  matrix,  $\mathbf{K}_0^{\text{even}}(\Delta)$ , given in equation (B.13). The condition for  $\mathbf{K}_0^{\text{even}}(\Delta)$  to have eigenvalue 1 is that

$$\det(\mathbf{K}_0^{\text{even}}(\Delta) - \mathbf{1}) = 0, \quad (5.5)$$

which determines the allowed values of  $\Delta$ .

We find the spectrum for  $\lambda = 1$  is 2.37666, 3, 3.70347, 5.23918, 5.57576, 7.22808, 7.57099. These approach  $2\Delta_\sigma + 2n = 1.57016 + 2n$  and  $2\Delta_\psi + 2n + 1 = 3.21492 + 2n$ , as expected. The scaling dimension of the lowest operator is plotted as a function of  $\lambda$  in Figure 5.<sup>7</sup> We also plot the scaling dimensions of the lowest several scalar primaries as a function of  $\lambda$  in Figure 6. As Figure 6 illustrates the spectrum is real for all values of  $\lambda$ .

We observe there exists an exactly marginal operator with  $\Delta = 3$ , for all  $\lambda$ . We expect that this corresponds to a mixture of  $\sigma^a \partial^2 \sigma^a$  and  $\bar{\psi}^i \not{\partial} \psi_i$ , which is redundant and vanishes by the equation of motion as in [41, 89].

In the limit  $\lambda \rightarrow \infty$  the scalar field becomes free, i.e.  $\Delta_\sigma = 1/2$ . The spectrum in the strict limit  $\lambda \rightarrow \infty$  includes only the roots 3.77189, 5.63427, 7.58896, which approach  $2\Delta_\psi + 2n + 1$ ; however for  $\lambda$  finite but arbitrarily large, there are also eigenvalues near 1, 3, 5, 7,  $\dots$  which approach  $2\Delta_\sigma + 2n$ .

For small  $\lambda$ , the operators whose scaling dimensions are close to  $2\Delta_\psi + 2n + 1$  are:

$$\Delta_0^A = 3 \quad (5.6)$$

and, for  $n \geq 1$ ,

$$\begin{aligned} \Delta_n^A &= 2\Delta_\psi + 2n + 1 + \frac{16(2n^2 + 3n - 1)}{3n(4n^3 + 12n^2 + 11n + 3)} \frac{\lambda^2}{\pi^4} \\ &+ \left( \frac{192(\log 2n + \gamma + 2) + 32}{27\pi^6 n^2} + O\left(\frac{1}{n^3}\right) \right) \lambda^3 + O(\lambda^4). \end{aligned} \quad (5.7)$$

---

<sup>7</sup>Both the lowest scaling dimension  $\Delta_0$  and its shadow  $\Delta'_0 = 3 - \Delta_0$  are above the unitary bound for all  $\lambda$ . Our analysis does not determine which is realized in the IR limit; however, as  $\lambda \rightarrow 0$ ,  $\Delta_0 \rightarrow 2^+ = 2\Delta_\sigma$ , in agreement with the GN model. Assuming the spectrum is a continuous function of  $\lambda$ , we conclude  $\Delta_0$  is the scaling dimension in the IR.

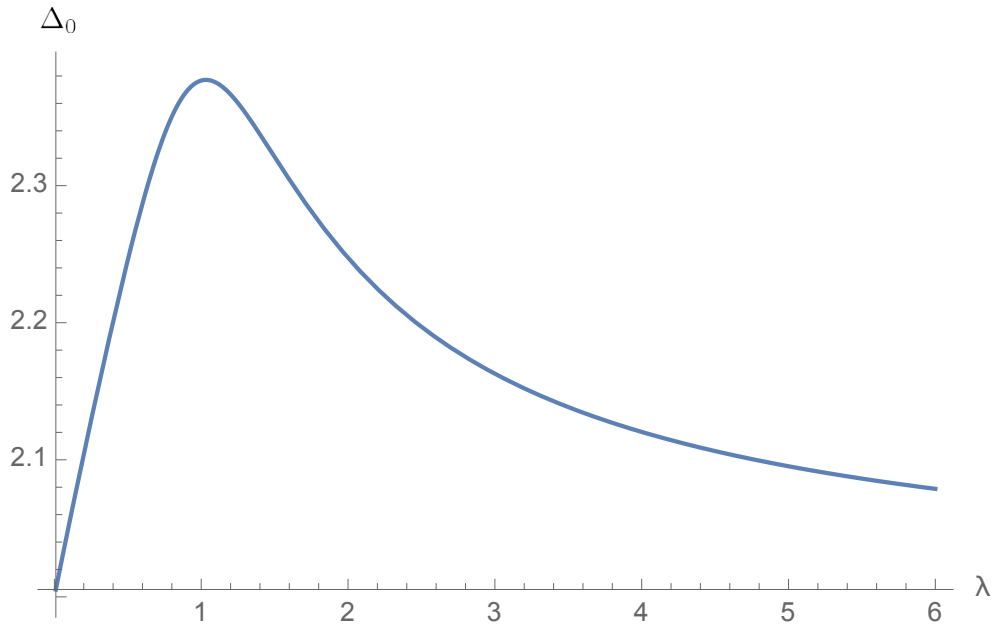


Figure 5: The scaling dimension  $\Delta_0(\lambda)$  of the lowest-dimension parity-even scalar as a function of  $\lambda$ .  $\Delta(\lambda)$  attains its maximum, 2.377 near  $\lambda = 1.03$ .

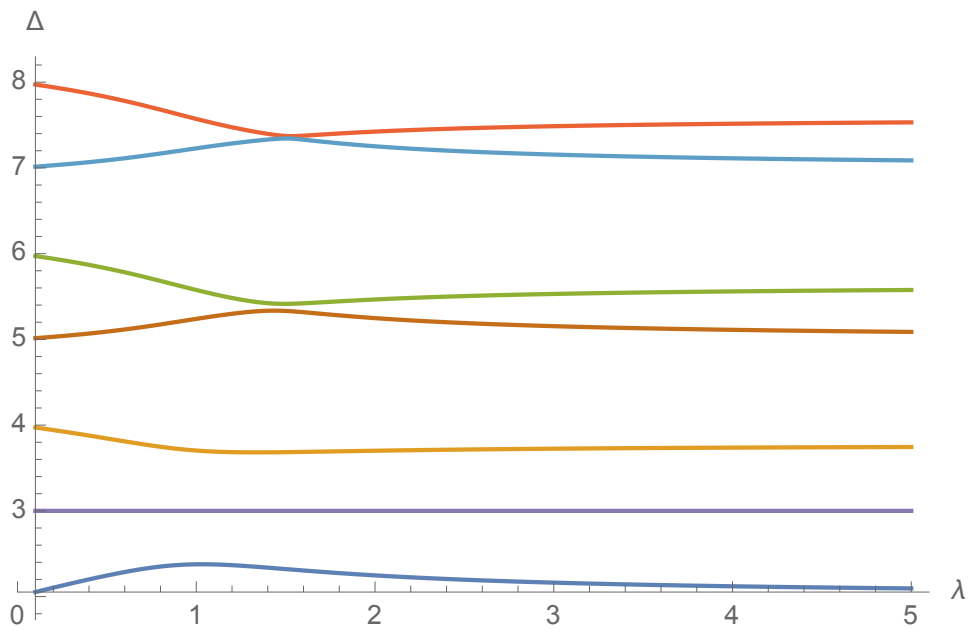


Figure 6: This figure shows the lowest 8 scaling dimensions of parity-even scalars in the spectrum as a function of  $\lambda$ . The kink in the graphs is, for large  $n$ , near the critical value of  $\lambda = 8/5$  for which  $2\Delta_\psi - 1 = 2\Delta_\sigma$ .

The operators corresponding whose scaling dimensions are close to  $2\Delta_\sigma + 2n$  are:

$$\Delta_0^B = 2\Delta_\sigma + \frac{8\lambda}{\pi^2} + \frac{(14208 - 928\pi^2)\lambda^3}{27\pi^6} + O(\lambda^4) \quad (5.8)$$

and

$$\begin{aligned} \Delta_n^B = 2\Delta_\sigma + 2n + \frac{64}{3\pi^4 n(n+1)(2n-1)(2n+1)} \lambda^2 + \\ \left( -\frac{384(\log 2n + \gamma - 4) + 128}{27\pi^6 n^4} + O\left(\frac{1}{n^5}\right) \right) \lambda^3 + O(\lambda^4). \end{aligned} \quad (5.9)$$

The order  $\lambda$  contribution to operators for which  $n > 0$  vanish (for both type A and type B), as expected, since these are double-trace operators in the theory when  $M = 1$ .

We also studied the anomalous dimensions when  $n$  is large, for arbitrary  $\lambda$ , and we found that

$$\lim_{n \rightarrow \infty} \gamma_n^A \sim n^{-2\Delta_\sigma}, \quad (5.10)$$

and

$$\lim_{n \rightarrow \infty} \gamma_n^B \sim \begin{cases} n^{-4\Delta_\psi} & \lambda \neq 8/5 \\ n^{-10/3} & \lambda = 8/5. \end{cases} \quad (5.11)$$

These are consistent with the  $O(\lambda^3)$  computations given above.

### 5.3 Higher-Spin Operators

We next compute the spectrum of higher spin operators. We focus our attention on leading twist higher-spin operators, i.e., those higher spin operators which become conserved currents when  $\lambda \rightarrow 0$ . These are all parity-even. This requires us to solve an equation of the form

$$\det(\mathbf{K}_s^{\text{even}}(\tau) - \mathbf{1}) = 0, \quad (5.12)$$

given in Appendix B. For  $s > 0$  and even,  $\mathbf{K}_s^{\text{even}}(\tau)$  is a  $3 \times 3$  matrix, while for  $s$  odd,  $\mathbf{K}_s^{\text{even}}(\tau)$  is a  $2 \times 2$  matrix.

The twists of leading-twist higher-spin operators are shown as a function of  $\lambda$  in the Figure 7. We first observe that, as expected, for all  $\lambda$ , there exists a spin-1 operator with twist 1, corresponding to a conserved  $U(1)$  current, and a spin-2 operator with twist 1, corresponding to a conserved stress-tensor.

For odd spins, the leading twists approach

$$\lim_{s \rightarrow \infty} \tau_s^{\text{min}} = 2\Delta_\psi - 1, \quad (5.13)$$

for all  $\lambda$ , while for even spins, the leading twists approach

$$\lim_{s \rightarrow \infty} \tau_s^{\text{min}} = \begin{cases} 2\Delta_\psi - 1 & \lambda \leq 8/5 \\ 2\Delta_\sigma & \lambda > 8/5 \end{cases}. \quad (5.14)$$

Define

$$\gamma_s = \tau_s - \lim_{s \rightarrow \infty} \tau_s^{\text{min}}. \quad (5.15)$$

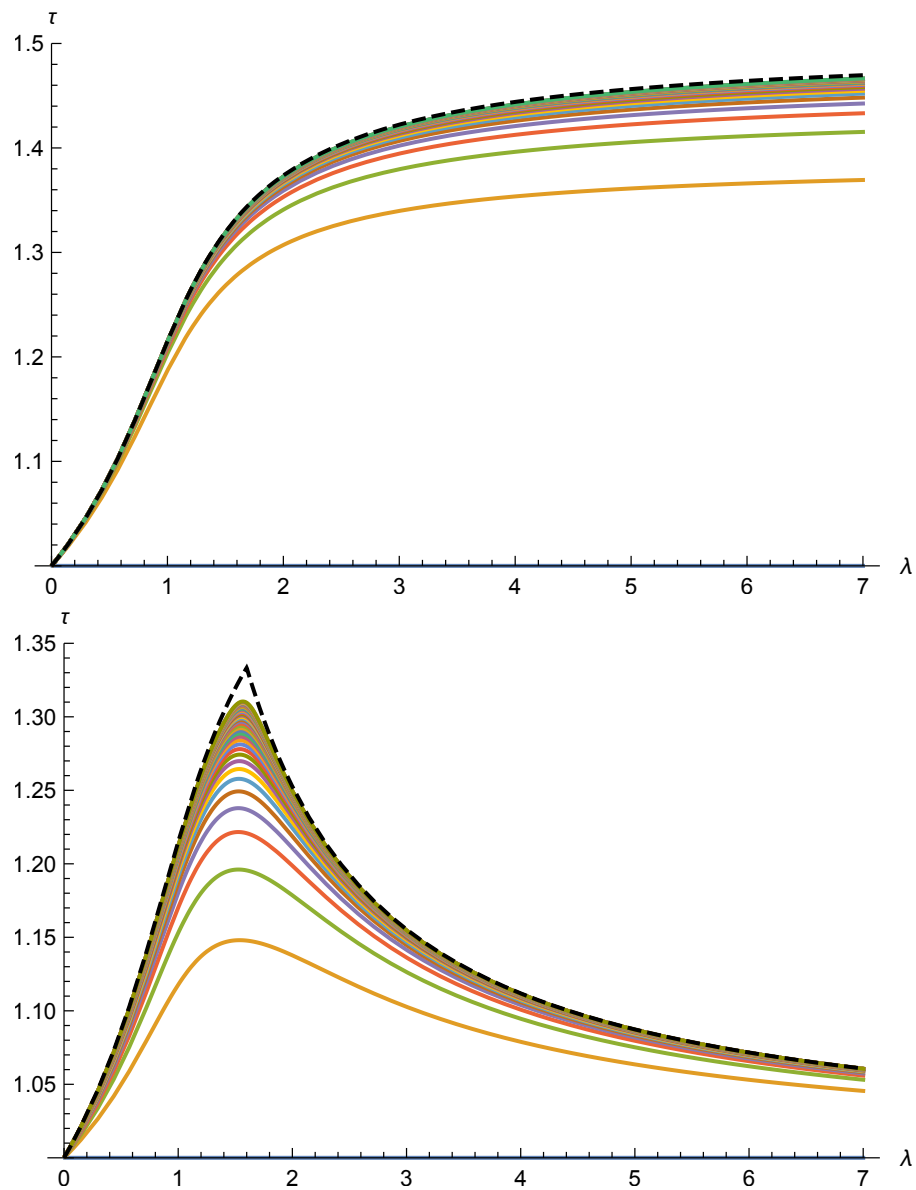


Figure 7: The spectrum of leading-twist operators of spin  $s$ , for  $s$  odd (above) and even (below), is shown as a function of  $\lambda$  for  $s = 1, \dots, 80$ . As  $s \rightarrow \infty$ , the anomalous dimensions approach the dashed line, and we expect a peak near  $\lambda = 8/5$ .

For small  $\lambda$ , these are given by,

$$\gamma_s = \begin{cases} -\frac{4\lambda}{\pi^2(2s-1)} + \frac{16\left(4s(2s-1)^2 H_{s-1} - (2s-1)^2(2s+1)(H_{s-\frac{3}{2}} + 2\log 2) - 2s(16s^2 - 22s + 13)\right)}{3\pi^4(2s-1)^3(2s+1)} \lambda^2 + O(\lambda^3) & s \text{ even} \\ -\frac{4\lambda}{\pi^2(4s^2-1)} - \frac{16\left((1-4s^2)^2(H_{s-\frac{3}{2}} + 2\log(2)) + 2(20s^4 - 13s^2 + 6s + 2)\right)}{3\pi^4(4s^2-1)^3} \lambda^2 + O(\lambda^3) & s \text{ odd} \end{cases} \quad (5.16)$$

We studied the behaviour of anomalous dimensions for large  $s$ .

For  $s$  even and  $\lambda < 8/5$ , we have

$$\gamma_s \sim -\frac{\cos(\pi\Delta_\psi)\Gamma\left(\frac{7}{2} - 3\Delta_\psi\right)\Gamma\left(\frac{7}{2} - \Delta_\psi\right)\Gamma\left(2\Delta_\psi - \frac{3}{2}\right)}{\pi^{3/2}(4(\Delta_\psi - 2)\Delta_\psi + 3)\Gamma(3 - 4\Delta_\psi)} s^{1-2\Delta_\psi}. \quad (5.17)$$

For  $s$  even and  $\lambda = 8/5$ , we have:

$$\gamma_s \sim -\frac{9\sqrt{\frac{3}{55}\Gamma\left(\frac{8}{3}\right)\Gamma\left(\frac{14}{3}\right)}}{4 \cdot 2^{5/6}\pi} s^{-2/3}. \quad (5.18)$$

For  $s$  even and  $\lambda > 8/5$ , we have:

$$\gamma_s \sim \frac{2\sin(4\pi\Delta_\psi)\cos(\pi\Delta_\psi)\Gamma(3 - 2\Delta_\psi)\Gamma\left(\frac{7}{2} - \Delta_\psi\right)\Gamma\left(2\Delta_\psi - \frac{1}{2}\right)\Gamma\left(3\Delta_\psi - \frac{7}{2}\right)}{\pi^{5/2}(2\Delta_\psi - 1)} s^{1-2\Delta_\psi}. \quad (5.19)$$

This agrees with the small  $\lambda$  behaviour. The asymptotic behaviour for the critical value of  $\lambda = 8/5$  is different than at other values of  $\lambda$  – note that, at this value,  $\Delta_\sigma = \frac{2}{3}$ , which is the smallest twist in the theory.

For  $s$  odd, we get a leading contribution proportional to  $s^{4\Delta_\psi-6} = s^{-2\Delta_\sigma}$  given by:

$$\gamma_s \sim -\frac{2(5 - 2\Delta_\psi)^2 \sin^2(2\pi\Delta_\psi)\Gamma(3 - 2\Delta_\psi)\Gamma(4 - 2\Delta_\psi)}{\pi^2(2\Delta_\psi - 1)^2} (4s)^{-2\Delta_\sigma}. \quad (5.20)$$

This is valid for all  $\lambda > 0$ . However, we find the subleading contribution is  $s^{2\Delta_\psi-4} = s^{-(\Delta_\sigma+1)}$ , which is close to the leading contribution for  $1 < \Delta_\psi < 5/4$ , making numerically verifying the exponent slightly difficult. In the limit  $\lambda \rightarrow 0$ , both the leading and subleading terms approach  $s^{-2+O(\lambda)}$ , so we do not expect agreement with the small  $\lambda$  expansion.

We also computed the twists of the higher-twist higher-spin operators, which we discuss in Appendix C.

## 5.4 Conformal Regge limit

While we have not computed out-of-time-ordered correlators of the model in flat space in  $d = 3$ , the value of  $s_*$  that solves

$$\det(\mathbf{K}_{s_*}^{\text{even}}(3/2 - s_*) - \mathbf{1}) = 0, \quad (5.21)$$

can be used to extract a Lyapunov exponent in a particular hyperbolic geometry, as explained in [44] via

$$\lambda_{hyp} = s_* - 1. \quad (5.22)$$

Here, to define the LHS of equation (5.21), we first assume the spin  $s$  is even, then analytically continue  $K_s^{\text{even}}(3/2 - s)$  to arbitrary complex spins. The hyperbolic Lyapunov exponent  $\lambda_{hyp}(\lambda)$  that we obtain from solving equation (5.21) is shown in Figure 8. We find a maximum at  $\lambda = 1.71$ , which is near the critical value of  $8/5$ .

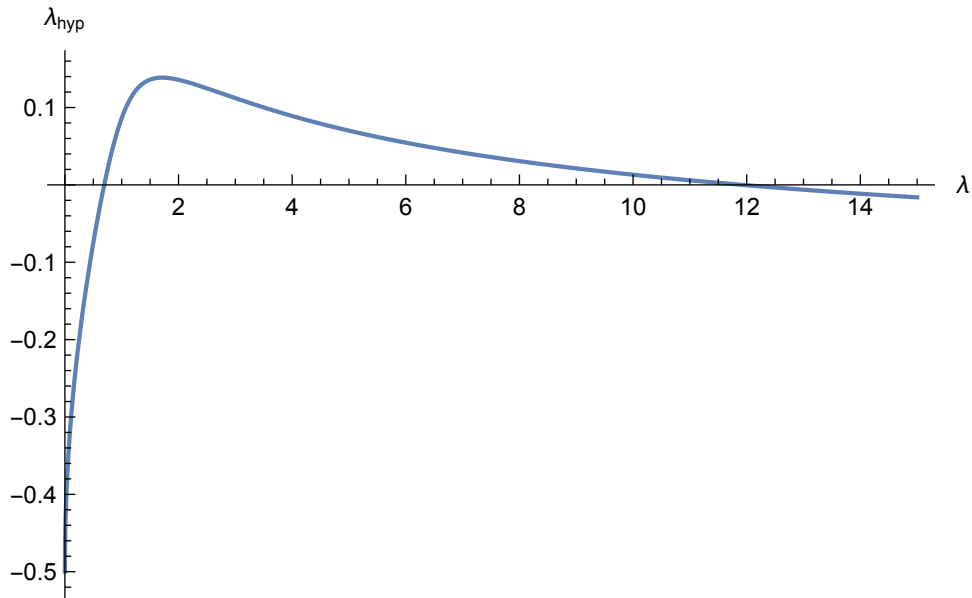


Figure 8: The hyperbolic Lyapunov exponent  $\lambda_{Hyp} = s_* - 1$  defined via the Regge limit of the parity-even higher spin kernel for even spins, as a function of  $\lambda$ . The maximum of  $\lambda_{hyp} = 0.139$  is attained at  $\lambda = 1.71$ .

## 6 Discussion

In this paper, we computed the spectrum of single-trace operators of an IR fixed point defined via a Gross-Neveu Yukawa model with a random coupling [51]. We found the model has purely real spectrum for all values of  $M/N$ . This result which strongly suggests the model is (to our knowledge, the first) well-defined non-supersymmetric CFT in  $d > 1$  that admits an SYK-like large  $N$  limit.

There are many avenues for future work – both in terms of computations and better understanding the potential physical applications of this theory. We hope to compute operator-product coefficients and central charges  $C_J$  and  $C_T$  in our model in the near future. We observed that there exists a critical value of  $M/N = 8/5$  where interactions appear to be strongest, and the large-spin behaviour of the theory is unusual – It would be interesting to better understand the physics of the conformal fixed point at this critical value of  $M/N$ .

When  $\lambda = 0$ , the model reduces to the GN fixed point, which is dual to a higher-spin gauge theory [7]. It is tempting to speculate that the disordered theory has a holographic dual that is a deformation of this higher-spin gauge theory – however, in the disordered theory, it appears impossible to eliminate non-singlet operators, by introducing a weakly interacting Chern-Simons gauge field [9, 10], so the existence of a holographic dual is uncertain. Even in the absence of a holographic dual, our theory is hopefully interesting as an example of a solvable non-supersymmetric interacting large  $N$  CFT in three dimensions.

In this paper, we focused on the conformal field theory in  $d = 3$  defined by the disordered GNY model. However, for  $\lambda > 1/2$ , it is also possible to define a conformal field theory in  $d = 2$ , as shown in [51], and we hope to study the spectrum of this theory in more detail in the future.

As noted in [51] several lattice realizations of the field theory in  $d = 3$  exist via models of fermions hopping on a honeycomb lattice. It is, therefore, natural to ask whether the disordered GNY model could have applications in condensed matter physics. Disordered one-dimensional

models with Yukawa interactions have been introduced as toy models of superconductivity – e.g., in [78, 79, 90–92]. Certain coupled SYK/tensor models have exhibited spontaneous breaking of  $\mathbb{Z}_2$  and  $U(1)$  symmetry [93, 94], which can be demonstrated directly via study of the Schwinger-Dyson equations in the melonic large  $N$  limit. While the model studied in the present work does not exhibit such symmetry-breaking, it would be interesting to search for a disordered Yukawa model (perhaps similar to the model in [95]) which does.<sup>8</sup>

## Acknowledgements

The author thanks I. Klebanov, R. Loganayagam, S. Minwalla, M. Rangamani, R. Sinha and S. Sachdev for discussions and comments on a draft of this publication. The author acknowledges support of a DST grant MTR/2018/0010077. The author also thanks International Centre for Theoretical Sciences, Bengaluru for hospitality where part of this work was completed.

## A Solving the gap equation from UV to IR

In this appendix, we solve the gap equation from weak to strong coupling for  $M \ll N$  very small, and  $M \gg N$ . From these results it seems natural to expect that a flow also exists for intermediate values of  $M/N$ .

Let  $F(p) = 1/f(p)$  and  $G(p) = -i\phi/g(p)$ . Here  $f(p)$  and  $g(p)$  are rationally invariant-functions of  $p^2$ . Note that  $[J] = 1$  in  $d = 3$ , so we expect these to be functions of the dimensionless quantity  $p/J$ .

The gap equations are:

$$f(p) = p^2 - Jd_\gamma \int \frac{d^d q}{(2\pi)^d} \frac{q^2 + q \cdot p}{g(q)g(p+q)} \quad (\text{A.1})$$

$$g(p) = p^2 + J\lambda \int \frac{d^d q}{(2\pi)^d} \frac{p \cdot q}{g(q)f(p-q)}. \quad (\text{A.2})$$

We will show these equations have a solution interpolating from the free UV solution to the IR solution at the extreme values of  $\lambda$ ,  $\lambda = 0$  and  $\lambda = \infty$ , which are easier to handle than intermediate values of  $\lambda$ . We have not attempted to numerically solve the gap equation for general  $\lambda$ .

The  $\lambda = 0$  solution is trivial, and can be obtained analytically. We have  $g^{(\lambda=0)}(p) = p^2$ , and  $f^{(\lambda=0)}(p)$  is given by

$$f^{(\lambda=0)}(p) = p^2 - Jd_\gamma \int \frac{d^d q}{(2\pi)^d} \frac{q^2 + q \cdot p}{q^2(p+q)^2} \quad (\text{A.3})$$

$$= p^2 - d_\gamma J \frac{2^{-d} \pi^{1-\frac{d}{2}} \csc\left(\frac{\pi d}{2}\right) \Gamma\left(\frac{d}{2}\right)}{\Gamma(d-1)} p^{d-2} \quad (\text{A.4})$$

$$\rightarrow_{d \rightarrow 3} p^2 + \frac{J}{8} p \quad (\text{A.5})$$

For  $\lambda \rightarrow \infty$ , we must solve the gap equation numerically. Let  $\tilde{J} = \lambda J$ . Then  $f^{(\lambda=\infty)}(p) = p^2$ , and  $g^{(\lambda=\infty)}(p)$  satisfies:

$$g^{(\lambda=\infty)}(p) = p^2 + \tilde{J} \int \frac{d^3 q}{(2\pi)^3} \frac{p \cdot q}{g^{(\lambda=\infty)}(p)(p-q)^2}. \quad (\text{A.6})$$

---

<sup>8</sup>The author thanks I. Klebanov for discussions on this point.

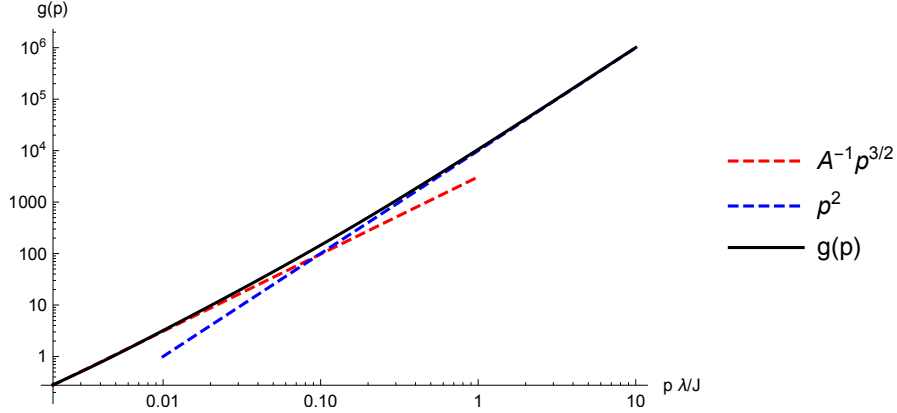


Figure 9: A numerical solution of the gap equation from UV to IR, for the case of  $\lambda \rightarrow \infty$  is shown above (the solid black line). It interpolates from  $g(p) \sim A^{-1}p^{3/2}$  (dashed red line) to  $g(p) \sim p^2$  (dashed blue line) as expected.

which we can write as

$$g^{(\lambda=\infty)}(p) = p^2 + \frac{\tilde{J}}{p(2\pi)^2} \int_0^\infty \frac{q^3 dq}{g^{(\lambda=\infty)}(p)} \mathcal{F}(q/p), \quad (\text{A.7})$$

where

$$\mathcal{F}(q) = \int_{-1}^1 dt \frac{t}{1+q^2-2qt}. \quad (\text{A.8})$$

We solve this equation iteratively, choosing the initial seed function as  $g_{\text{seed}}(p) = p^2 + A^{-1}p^{3/2}$ , where  $A^2 = \frac{10\pi}{3J}$ . Within a few iterations, this converged to the numerical function plotted in Figure 9.

## B Details of the computation of the spectrum

### B.1 Conformally-Invariant Three-Point functions

Let  $\mathcal{O}_{\tau,s}^{\text{odd/even}}(x, z)$  be a parity-odd/parity-even operator with spin  $s$  and twist  $\tau = \Delta_{\mathcal{O}} - s$ . There are two allowed forms [85] for conformally-invariant three-point correlation functions

$$\langle \bar{\lambda}_1 \psi(x_1) \mathcal{O}_{\tau,s}^{\text{odd/even}}(x_3, z_3) \bar{\psi}(x_2) \lambda_2 \rangle,$$

which are:

$$\langle \bar{\lambda}_1 \psi(x_1) \mathcal{O}_{\tau,s}^{\text{odd}}(x_3, z_3) \bar{\psi}(x_2) \lambda_2 \rangle = \frac{1}{x_{31}^\tau x_{12}^{2\Delta_\psi - 1 - \tau} x_{23}^\tau} (b_1(S_3/P_3)Q_3^s + b_2(S_1/P_1)P_2Q_3^{s-1}), \quad (\text{B.1})$$

for parity-odd operators, and

$$\langle \bar{\lambda}_1 \psi(x_1) \mathcal{O}_{\tau,s}^{\text{even}}(x_3, z_3) \bar{\psi}(x_2) \lambda_2 \rangle = \frac{1}{x_{31}^\tau x_{12}^{2\Delta_\psi - 1 - \tau} x_{23}^\tau} (a_1 P_3 Q_3^s + a_2 P_1 P_2 Q_3^{s-1}), \quad (\text{B.2})$$

for parity-even operators. Here  $Q_i$ ,  $P_i$  and  $S_i$  are defined in [85], as,

$$P_3 = \bar{\lambda}_1 \not{x}_{12}^2 \lambda_2, \quad Q_3 = 2z_3 \cdot \left( \frac{x_{32}}{x_{32}^2} - \frac{x_{31}}{x_{31}^2} \right), \quad S_3/P_3 = i\bar{\lambda}_2 \not{x}_{23} \not{x}_{31} \lambda_1 / (|x_{12}| |x_{23}| |x_{31}|). \quad (\text{B.3})$$



For  $s = 0$ , the second term in each of the two above expressions should be omitted, and there is only one allowed form for the three-point function.

The correlation function  $\langle \sigma(x_1)\sigma(x_2)\mathcal{O}_{\tau,s}^{odd} \rangle$  vanishes. The only allowed form for a conformally-invariant correlation function  $\langle \sigma(x_1)\sigma(x_2)\mathcal{O}_{\tau,s}^{even}(x_3, z_3) \rangle$  is

$$\langle \sigma(x_1)\sigma(x_2)\mathcal{O}_{\tau,s}^{even}(x_3) \rangle = \frac{c_1 Q_3^s}{x_{12}^{2\Delta_\sigma - \tau} x_{23}^\tau x_{31}^\tau}. \quad (\text{B.4})$$

It is convenient to take the limit  $x_3 \cdot z_3 = 0$  and  $x_3 \rightarrow \infty$ , which can be obtained by a conformal transformation. This makes  $Q_3 \rightarrow 2z_3 \cdot \frac{x_{21}}{x_3^2}$ . We also rescale the correlation functions by a factor of  $x_3^{2\tau+2s}$ . In this limit the allowed forms for the correlation functions become:

$$v_{a_1} = \bar{\lambda}_1 \not{x}_{12} \lambda_2 \frac{(x_{12} \cdot \epsilon)^s}{|x_{12}|^{-\tau+1+2\Delta_\psi}} \quad (\text{B.5})$$

$$v_{a_2} = \bar{\lambda}_1 \not{\epsilon} \lambda_2 \frac{(x_{12} \cdot \epsilon)^{s-1}}{|x_{12}|^{-\tau-1+2\Delta_\psi}} \quad (\text{B.6})$$

$$v_{b_1} = \bar{\lambda}_1 \lambda_2 \frac{(x_{12} \cdot \epsilon)^s}{|x_{12}|^{2\Delta_\psi - \tau}} \quad (\text{B.7})$$

$$v_{b_2} = \bar{\lambda}_1 \not{\epsilon} \not{x}_{12} \lambda_2 \frac{(x_{12} \cdot \epsilon)^{s-1}}{|x_{12}|^{2\Delta_\psi - \tau}} \quad (\text{B.8})$$

$$v_{c_1} = \frac{(x_{12} \cdot \epsilon)^s}{|x_{12}|^{2\Delta_\sigma - \tau}} \quad (\text{B.9})$$

We may prefer to choose a different basis for the parity-odd three-point functions, by defining,

$$v'_{b_2} = \bar{\lambda}_1 (\not{\epsilon} \not{x}_{12} - \not{x}_{12} \not{\epsilon}) \lambda_2 \frac{(x_{12} \cdot z)^{s-1}}{|x_{12}|^{2\Delta_\psi - \tau}}, \quad (\text{B.10})$$

which, it turns out, does not mix with  $v_{b_1}$ .

## B.2 Integration kernel

Using the above results, we compute the integration kernel as usual.

For parity-even spin- $s$  operators, the diagrammatic equation in Figure 3 translates into the eigenvalue equation for the coefficients  $a_1$ ,  $a_2$  and  $c_1$  defined in equations (B.2) and (B.4):

$$\begin{pmatrix} a_1 \\ a_2 \\ c_1 \end{pmatrix} = \mathbf{K}_s^{\text{even}}(\tau) \begin{pmatrix} a_1 \\ a_2 \\ c_1 \end{pmatrix}. \quad (\text{B.11})$$

We must determine the values of  $\tau$  for which the  $3 \times 3$  matrix  $\mathbf{K}_s^{\text{even}}(\tau)$  has an eigenvalue equal to 1. Similarly, for the spectrum of parity-odd spin- $s$  operators, Figure 3 translates into an eigenvalue equation for a  $2 \times 2$  matrix  $\mathbf{K}_s^{\text{odd}}(\tau)$ . For parity-even spin zero operators, Figure 3 translates into an eigenvalue equation for another  $2 \times 2$  matrix,  $\mathbf{K}_0^{\text{even}}(\tau)$ . For parity odd spin-zero operators, Figure 3 translates into a conventional integration kernel, i.e., a  $1 \times 1$  matrix,  $K_0^{\text{odd}}(\tau)$ .

The 9 entries of the integration kernel matrix for spin- $s$  parity-even operators are given by

$$\mathbf{K}_s^{\text{even}}(\tau) = \begin{pmatrix} K_{a_1, a_1}[v_{a_1}(y_1, y_2)]/v_{a_1}(x_1, x_2) & K_{a_1, a_2}[v_{a_2}(y_1, y_2)]/v_{a_1}(x_1, x_2) & K_{a_1, c}[v_c(y_1, y_2)]/v_{a_1}(x_1, x_2) \\ K_{a_2, a_1}[v_{a_1}(y_1, y_2)]/v_{a_2}(x_1, x_2) & K_{a_2, a_2}[v_{a_2}(y_1, y_2)]/v_{a_2}(x_1, x_2) & K_{a_2, c}[v_c(y_1, y_2)]/v_{a_2}(x_1, x_2) \\ K_{c, a_1}[v_{a_1}(y_1, y_2)]/v_c(x_1, x_2) & K_{c, a_2}[v_{a_2}(y_1, y_2)]/v_c(x_1, x_2) & K_{c, c}[v_c(y_1, y_2)]/v_c(x_1, x_2) \end{pmatrix}, \quad (\text{B.12})$$

for  $s > 0$ . For  $s$  odd, the last row and last column of this matrix vanish identically. For  $s = 0$ , the second row and second column of the matrix are not present.

The 4 entries of the integration kernel matrix for spin-zero parity-even operators are given by

$$\mathbf{K}_0^{\text{even}}(\tau) = \begin{pmatrix} K_{a_1, a_1}[v_{a_1}(y_1, y_2)]/v_{a_1}(x_1, x_2) & K_{a_1, c}[v_c(y_1, y_2)]/v_{a_1}(x_1, x_2) \\ K_{c, a_1}[v_{a_1}(y_1, y_2)]/v_c(x_1, x_2) & K_{c, c}[v_c(y_1, y_2)]/v_c(x_1, x_2) \end{pmatrix}, \quad (\text{B.13})$$

for  $s = 0$ .

In the above matrices, we have:

$$\begin{aligned} & K_{a_1, a_1}[v_{a_1}(y_1, y_2)] + K_{a_2, a_1}[v_{a_1}(y_1, y_2)] \\ &= J\lambda \int d^d y_1 d^d y_2 \bar{\lambda}_1 G(x_1, y_1) \not{y}_{12} G(y_2, x_2) \lambda_2 \frac{(y_{12} \cdot \epsilon)^s}{y_{12}^{-\tau+1+2\Delta_\psi}} F(y_1, y_2), \end{aligned} \quad (\text{B.14})$$

$$K_{c, a_1}[v_{a_1}(y_1, y_2)] = -J \int d^d y_1 d^d y_2 F(x_1, y_1) F(y_2, x_2) \text{tr} \left( \not{y}_{12} G(y_2, y_1) \right) \frac{(y_{12} \cdot \epsilon)^s}{y_{12}^{-\tau+1+2\Delta_\psi}}, \quad (\text{B.15})$$

$$\begin{aligned} & K_{a_1, a_2}[v_{a_2}(y_1, y_2)] + K_{a_2, a_2}[v_{a_2}(y_1, y_2)] \\ &= J\lambda \int d^d y_1 d^d y_2 \bar{\lambda}_1 G(x_1, y_1) \not{\epsilon} G(y_2, x_2) \lambda_2 \frac{(y_{12} \cdot \epsilon)^{s-1}}{y_{12}^{-\tau-1+2\Delta_\psi}} F(y_1, y_2), \end{aligned} \quad (\text{B.16})$$

$$K_{c, a_2}[v_{a_2}(y_1, y_2)] = -J \int d^d y_1 d^d y_2 F(x_1, y_1) F(y_2, x_2) \text{tr} \left( \not{\epsilon} G(y_2, y_1) \right) \frac{(y_{12} \cdot \epsilon)^{s-1}}{y_{12}^{-\tau-1+2\Delta_\psi}}, \quad (\text{B.17})$$

$$\begin{aligned} & K_{a_1, c}[v_c(y_1, y_2)] + K_{a_2, c}[v_c(y_1, y_2)] \\ &= J\lambda \int d^d y_1 d^d y_2 \bar{\lambda}_1 G(x_1, y_1) G(y_1, y_2) G(y_2, x_2) \lambda_2 \frac{(y_{12} \cdot \epsilon)^s}{y_{12}^{-\tau+2\Delta_\sigma}}, \end{aligned} \quad (\text{B.18})$$

and

$$K_{c, c}[v_c(y_1, y_2)] = 0. \quad (\text{B.19})$$

For parity-odd spin  $s$  operators, we have

$$\mathbf{K}_s^{\text{odd}}(\tau) = \begin{pmatrix} K_{b_1, b_1}[v_{b_1}(y_1, y_2)]/v_{b_1}(x_1, x_2) & K_{b_1, b_2}[v_{b_2}(y_1, y_2)]/v_{b_1}(x_1, x_2) \\ K_{b_2, b_1}[v_{b_1}(y_1, y_2)]/v_{b_2}(x_1, x_2) & K_{b_2, b_2}[v_{b_2}(y_1, y_2)]/v_{b_2}(x_1, x_2) \end{pmatrix}, \quad (\text{B.20})$$

where,

$$\begin{aligned} & K_{b_1, b_1}[v_{b_1}(y_1, y_2)] + K_{b_2, b_1}[v_{b_1}(y_1, y_2)] \\ &= J\lambda \int d^d y_1 d^d y_2 \bar{\lambda}_1 G(x_1, y_1) G(y_2, x_2) \lambda_2 \frac{(y_{12} \cdot \epsilon)^s}{y_{12}^{-\tau+2\Delta_\psi}} F(y_1, y_2), \end{aligned} \quad (\text{B.21})$$

and

$$\begin{aligned} & K_{b_1, b_2}[v_{b_2}(y_1, y_2)] + K_{b_2, b_2}[v_{b_2}(y_1, y_2)] \\ &= J\lambda \int d^d y_1 d^d y_2 \bar{\lambda}_1 G(x_1, y_1) \not{y}_{12} G(y_2, x_2) \lambda_2 \frac{(y_{12} \cdot \epsilon)^{s-1}}{y_{12}^{-\tau+2\Delta_\psi}} F(y_1, y_2). \end{aligned} \quad (\text{B.22})$$

$\mathbf{K}_s^{\text{odd}}(\tau)$  is a  $2 \times 2$  matrix for  $s > 0$ . For parity-odd spin 0 operators, there is no mixing and only one allowed form for the three-point function. The integration kernel  $K_0^{\text{odd}}(\tau)$  is therefore a  $1 \times 1$  matrix:

$$K_0^{\text{odd}}(\tau) = K_{b_1, b_1}[v_{b_1}(y_1, y_2)]/v_{b_1}(x_1, x_2). \quad (\text{B.23})$$

Before we proceed, let us point out a technical complication. Unlike the usual SYK model, or the higher-dimensional bosonic variants, we find that there are multiple allowed forms for the three-point correlation functions. Like mixing, as discussed in [44,50,47], this means the integration kernel is a matrix – and the allowed scaling dimensions are those for which is an 1 eigenvalue of the matrix. When two operators mix we expect two linearly independent mixtures to exist that have well-defined scaling dimensions. This is reflected in the fact that the calculation of the integration kernel involves diagonalizing a two-by-two matrix and eventually leads to two set of spectra, both of which are physical. However, suppose there are multiple allowed forms for the three-point correlation function – for simplicity, assume that there are  $n$  allowed forms for the three point function and no mixing. In the actual IR fixed point, only one three-point function would be realized, which correspond to one of the eigenvectors of an  $n \times n$  integration-kernel matrix, with eigenvalue 1. The other eigenvectors, and their associated eigenvalues, would be spurious. We therefore determine  $n$  candidate scaling dimensions for each operator, without identifying which of one these scaling dimensions is actually realized. Luckily, we are able to resolve this ambiguity by assuming the spectrum of the theory is a continuous function of  $\lambda$ . This complication does not affect spin-zero operators.

### B.3 Numerically solving for the allowed scaling dimensions

To determine the allowed scaling dimensions of parity-odd scalars, we must determine the values of  $\tilde{\Delta}$  for which  $K_0^{\text{odd}}(\tilde{\Delta}) = 1$ . This gives rise to

$$-\frac{\Gamma\left(\frac{1}{2}(d-2\Delta_\psi+1)\right)\Gamma\left(d-\Delta_\psi+\frac{1}{2}\right)\Gamma\left(\Delta_\psi-\frac{\tilde{\Delta}}{2}\right)\Gamma\left(-\frac{d}{2}+s+\Delta_\psi+\frac{\tilde{\Delta}}{2}\right)}{\Gamma\left(\Delta_\psi+\frac{1}{2}\right)\Gamma\left(-\frac{d}{2}+\Delta_\psi+\frac{1}{2}\right)\Gamma\left(d-\Delta_\psi-\frac{\tilde{\Delta}}{2}\right)\Gamma\left(\frac{1}{2}(d+2s-2\Delta_\psi+\tilde{\Delta})\right)}=1. \quad (\text{B.24})$$

We carry out this computation numerically for  $d = 3$ , as illustrated in Figures 10 and 11 for  $\lambda = 1$  and  $\lambda = \infty$  respectively. These figures illustrate that the spectrum is real for these values of  $\lambda$ , and we established analytically that the spectrum is real for small  $\lambda$ . We also determined the spectrum for numerous intermediate values of  $\lambda$  and found that it is real as well.

## C Higher-twist spin- $s$ operators in $d = 3$

### C.1 Parity-Even Higher-Spin Operators

The calculation leading to the numerical spectrum for  $s = 1, 2$  and  $\lambda = 1$  is shown in Figure 12. The plots for higher-spin operators are similar, except that the leading twist is no longer at  $\tau = 1$ .

From Figure 12, we see that, for operators of both leading and subleading twist, there is no ambiguity in the spectrum. The spectrum of operators of sub-leading twists are shown in Figure 13 as a function of  $\lambda$ .

However, as discussed in Appendix B, there is an ambiguity in determining the higher-twist higher-spin operators. Because there are two allowed forms for the correlation function involving two fermions and a spin- $s$  operator, we find two values of  $\tau_{s,n}^A$  for which  $K = 1$ , for each  $s > 0$  and  $n > 0$ . These approach  $2\Delta_\psi - 1$  from above and below as  $n \rightarrow \infty$  or  $s \rightarrow \infty$ , so we denote them as  $\tau_{s,n}^{A+}$  and  $\tau_{s,n}^{A-}$  respectively. Only one of  $\tau_{s,n}^{A\pm}$  is physical. Because there is only one allowed form for  $\langle \sigma \sigma J_s \rangle$ , no such ambiguity is present for  $\tau_{s,n}^B$ . This can be seen in in Figure 12.

We resolve this ambiguity by demanding anomalous dimensions are continuous functions of  $\lambda$ .

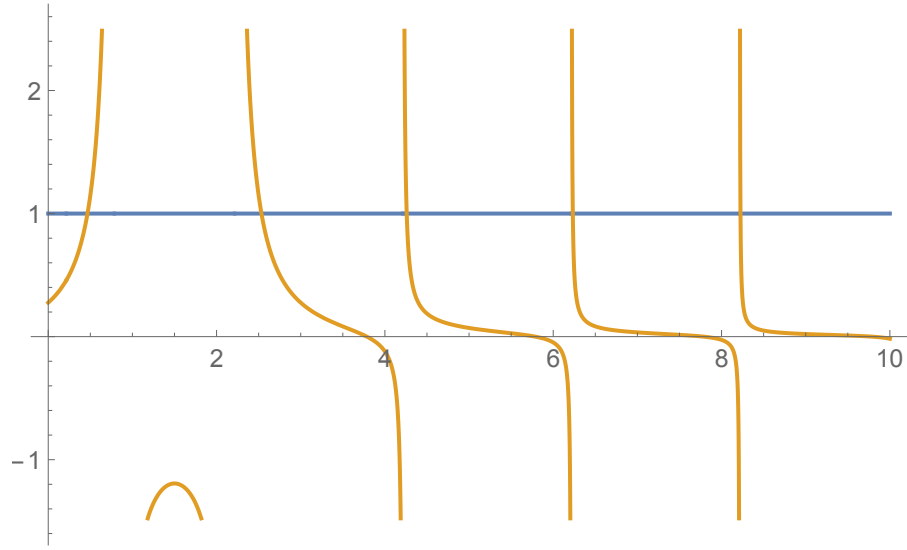


Figure 10: Computing the spectrum of spin-zero parity-odd scalars in  $d = 3$  for  $\lambda = 1$  by solving equation (5.1). For other values of  $\lambda$ , the calculation is very similar, and we find lowest twist parity-odd scalar has real scaling dimension for all  $\lambda$ , in contrast to other non-supersymmetric melonic theories, such as [49].

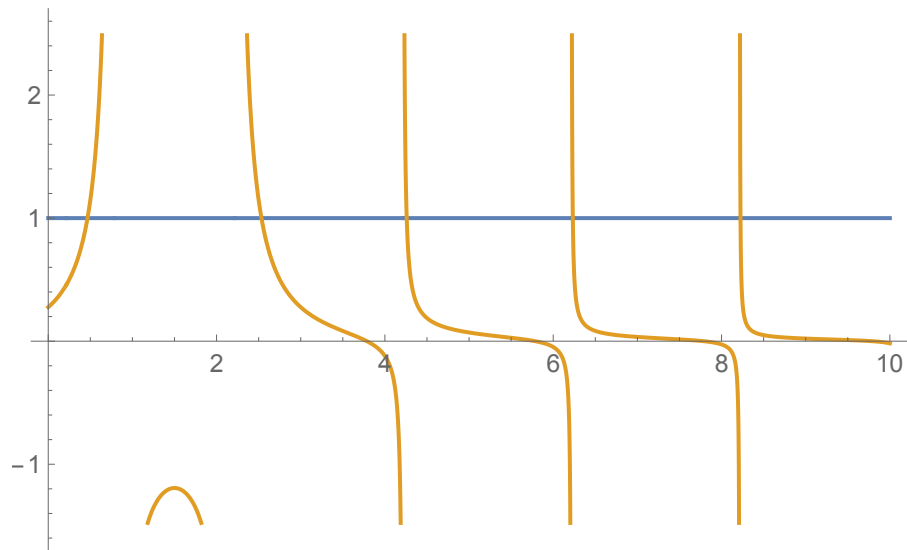


Figure 11: Computing the spectrum of spin-zero parity-odd scalars in  $d = 3$  for  $\lambda = \infty$ .

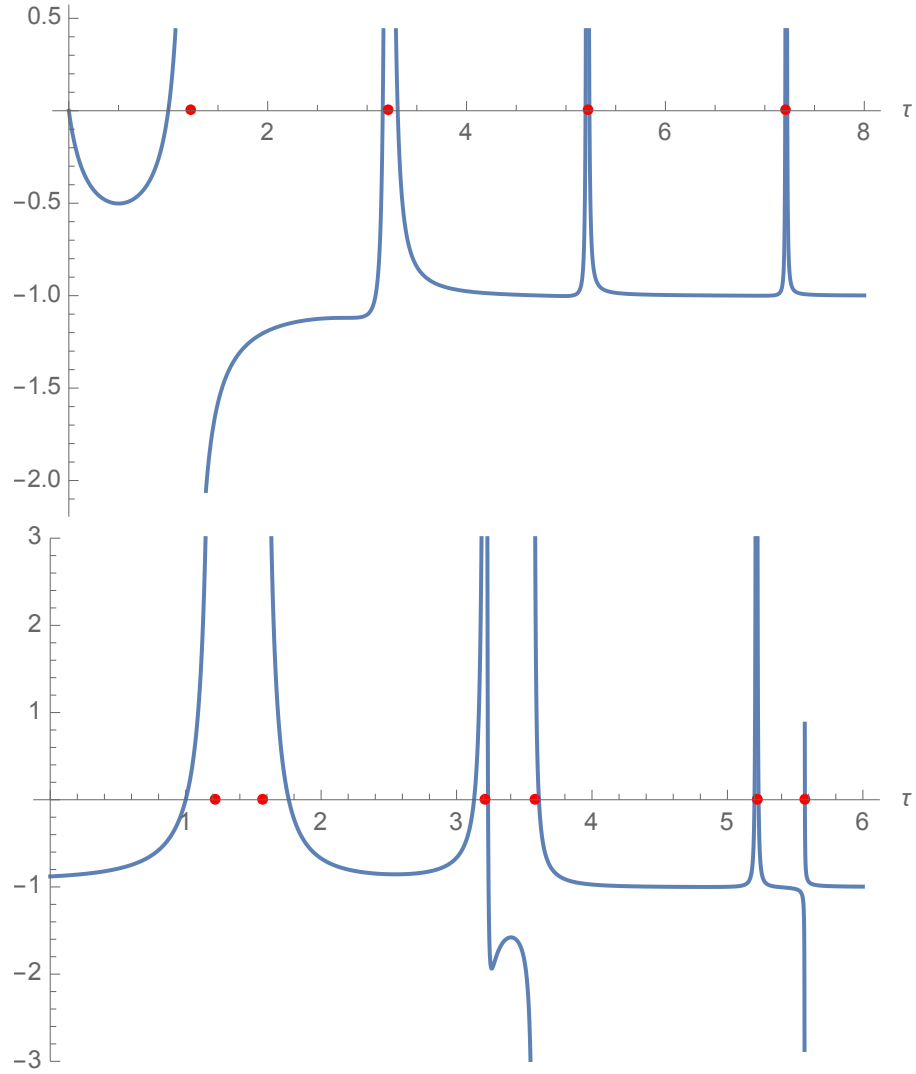


Figure 12: Determining the spectrum of parity-even single-trace spin-1 (above) and spin-2 (below) operators for  $\lambda = 1$ . Red dots denote asymptotic values of twists, approached as  $n \rightarrow \infty$ .

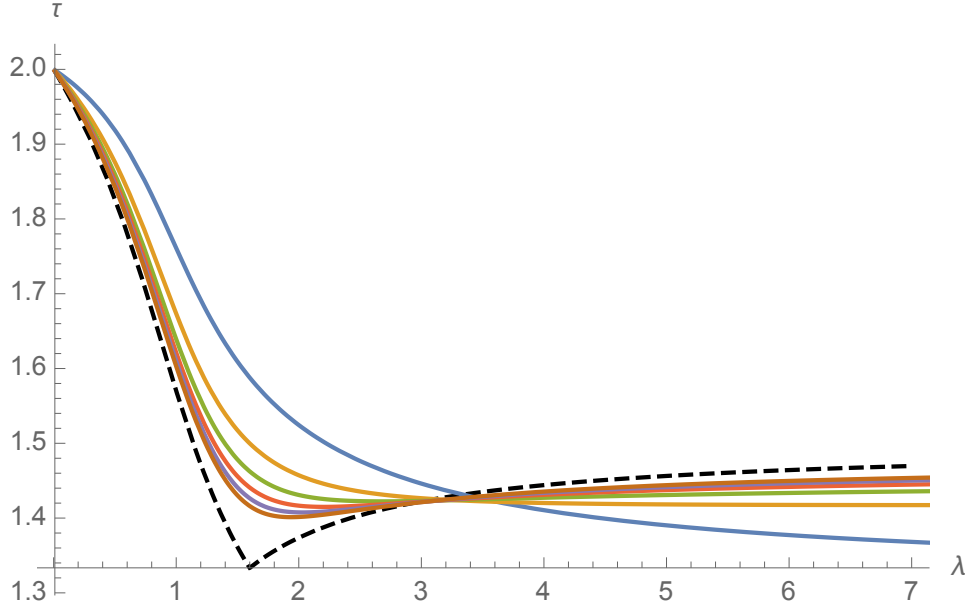


Figure 13: The anomalous dimensions of the even spin higher-spin operators of sub-leading twist. The dashed-line is the asymptotic value approached as  $s \rightarrow \infty$ . For sufficiently large  $\lambda$  these are monotonically increasing functions of  $s$ .

We find that that the functions

$$\tau_{s,n}^{(1)}(\lambda) = \begin{cases} \tau_{s,n}^{A-}(\lambda) & \lambda < \lambda_* \\ \tau_{s,n}^B(\lambda) & \lambda > \lambda_* \end{cases} \quad (\text{C.1})$$

and

$$\tau_{s,n}^{(2)}(\lambda) = \begin{cases} \tau_{s,n}^B(\lambda) & \lambda < \lambda_* \\ \tau_{s,n}^{A+}(\lambda) & \lambda > \lambda_* \end{cases} \quad (\text{C.2})$$

are continuous functions of  $\lambda$ . Therefore

$$\tau_{n,s}^A = \begin{cases} \tau_{n,s}^{A-} & \lambda < \lambda_* \\ \tau_{n,s}^{A+} & \lambda > \lambda_* \end{cases}. \quad (\text{C.3})$$

## C.2 Parity-odd higher spin operators

The same ambiguity arises for parity odd higher-spin operators. In this case, it is possible to explicitly choose a basis – formed by  $v_{b_1}$  and  $v'_{b_2}$  in equations (B.7) and (B.10) – for correlation functions that diagonalizes the  $2 \times 2$  integration kernel matrix for all  $\Delta_\psi$ ,  $\tau$  and  $s$ . There are therefore two integration kernels

$$\tilde{K}_s^+(\tilde{\tau}) = -\frac{\Gamma(\frac{1}{2}(d-2\Delta_\psi+1))\Gamma(d-\Delta_\psi+\frac{1}{2})\Gamma(\Delta_\psi-\frac{\tau}{2})\Gamma(-\frac{d}{2}+s+\Delta_\psi+\frac{\tau}{2})}{\Gamma(\Delta_\psi+\frac{1}{2})\Gamma(-\frac{d}{2}+\Delta_\psi+\frac{1}{2})\Gamma(d-\Delta_\psi-\frac{\tau}{2})\Gamma(\frac{1}{2}(d+2s-2\Delta_\psi+\tau))}, \quad (\text{C.4})$$

and

$$\tilde{K}_s^-(\tilde{\tau}) = \frac{2\Gamma(\frac{1}{2}(d-2\Delta_\psi+1))\Gamma(d-\Delta_\psi+\frac{1}{2})\Gamma(\Delta_\psi-\frac{\tau}{2})\Gamma(-\frac{d}{2}+s+\Delta_\psi+\frac{\tau}{2})}{\Gamma(\Delta_\psi+\frac{1}{2})\Gamma(-\frac{d}{2}+\Delta_\psi+\frac{1}{2})\Gamma(d-\Delta_\psi-\frac{\tau}{2})\Gamma(\frac{1}{2}(d+2s-2\Delta_\psi+\tau))}. \quad (\text{C.5})$$

The eigenvector corresponding to  $\tilde{K}_s^+$  is  $v_{b_1}$ , is also valid for  $s = 0$ , while the eigenvector corresponding to  $\tilde{K}_s^-$  is  $v'_{b_2}$  and requires  $s \geq 1$ .

The equations  $\tilde{K}_s^\pm(\tilde{\tau}) = 1$  have solutions  $\tilde{\tau}_{n,s}^+$  and  $\tilde{\tau}_{n,s}^-$  for each integer  $n \geq 0$ .  $\tilde{\tau}_{n,s}^+$  and  $\tilde{\tau}_{n,s}^-$  approach  $2\Delta_\psi + 2n$  from above and below, respectively, as  $n \rightarrow \infty$  or  $s \rightarrow \infty$ .

When we solve these equations numerically, we find that  $\tilde{\tau}_{1,0}^-(\lambda)$  becomes complex near  $\lambda = 6.375$ , while  $\tilde{\tau}_{s,0}^+$  remains real for all  $\lambda$ . Hence, it is important to know whether  $\tilde{\tau}_{s,n}^+$  or  $\tilde{\tau}_{s,n}^-$  is realized in the IR limit.

We carried out a perturbative Feynman diagram calculation of the anomalous dimension of  $\overleftrightarrow{\psi} \partial (\cdot z)^s \psi$  to first order in  $\lambda$  for odd  $s$ . This is very similar to calculating  $1/N$  corrections to the GN vector model, we use the IR propagators at  $\lambda = 0$ :  $F(p) = \frac{8\lambda}{Jp}$  and  $G(p) = G_0(p)$ , and, keep track of index contractions arising from disorder-averaging – which means we keep only melonic diagrams. There is only one diagram that contributes for odd  $s$  (other than the self-energy of the fermion) which is given by:

$$- \int \frac{d^3q}{(2\pi)^3} \frac{8\lambda}{q(p+q)^2} ((p+q) \cdot z)^s \rightarrow - \frac{4}{(2s+1)\pi^2} \lambda \log \Lambda. \quad (\text{C.6})$$

We find that  $\tilde{\tau}_{s,0} = 2\Delta_\psi + \frac{4}{(2s+1)\pi^2} \lambda + O(\lambda^2)$ , for odd  $s$ , which matches  $\tilde{\tau}_{s,0}^+$  obtained from solving  $\tilde{K}_s^+ = 1$ . Assuming anomalous dimensions are continuous functions of  $\lambda$ , we conclude that  $\tilde{\tau}_{s,0}^+$  are the physically realized twists for the leading twist parity-odd higher spin operators, and our spectrum is free from any operators of complex scaling dimension for all  $\lambda$ . If we assume  $\tilde{\tau}_{s,n}$  are monotonic functions of  $n$ , this also implies that  $\tau_{s,n}^+$  are the physically realized twists for  $n > 0$  – to confirm this expectation would require an order  $\lambda^2$  perturbative calculation. However, for  $n > 0$ , both  $\tau_{s,n}^+$  and  $\tau_{s,n}^-$  are real so distinguishing between them is not essential for the main conclusion of the paper.

For small  $\lambda$ , we find that

$$\begin{aligned} \tilde{\gamma}_{s,0} &= \frac{4}{\pi^2(2s+1)} \lambda \\ &+ \frac{16 \left( 9(2s+1)^2 H_{s-\frac{1}{2}} + 80s^3 + 12s^2(13 + \log(64)) + 12s(8 + \log(64)) - 8 + 9 \log(4) \right)}{27\pi^4(2s+1)^3} \lambda^2 + O(\lambda^3) \end{aligned} \quad (\text{C.7})$$

and

$$\begin{aligned} \tilde{\gamma}_{s,n} &= \frac{16}{3\pi^4 n(2n+2s+1)} \lambda^2 \\ &+ \frac{8 \left( 6n(2n+2s+1) \left( H_{n+s-\frac{1}{2}} + H_{n-1} + \log(4) \right) + 26n(2n+2s+1) + 9 \right)}{27\pi^6 n^2 \left( n + s + \frac{1}{2} \right)^2} \lambda^3 + O(\lambda^4) \\ &\sim_{n \rightarrow \infty} \frac{8}{3\pi^4 n^2} \lambda^2 + \frac{32(6 \log(n) + 6\gamma + 13 + 3 \log(4))}{27\pi^6 n^2} \lambda^3 + O(\lambda^3) \\ &\sim_{s \rightarrow \infty} \frac{8}{3\pi^4 ns} \lambda^2 + \frac{32(3H_{n-1} + 3 \log(s) + 3\gamma + 13 + 3 \log(4))}{27\pi^6 ns} \lambda^3 + O(\lambda^4). \end{aligned} \quad (\text{C.8})$$

At large  $s$ , we find,

$$\tilde{\gamma}_{s,n} \sim \frac{2^{4\Delta_\psi - 5} (2\Delta_\psi - 5) \sin(2\pi\Delta_\psi) \Gamma(4 - 2\Delta_\psi)}{\pi(1 - 2\Delta_\psi)} s^{-\Delta_\sigma}, \quad (\text{C.9})$$

and at large  $n$ ,

$$\tilde{\gamma}_{s,n} \sim \frac{2^{4\Delta_\psi - 5} (5 - 2\Delta_\psi) \sin^2(2\pi\Delta_\psi) \Gamma(3 - 2\Delta_\psi) \Gamma(4 - 2\Delta_\psi)}{\pi^2(2\Delta_\psi - 1)} n^{-2\Delta_\sigma}. \quad (\text{C.10})$$

## D Spectrum in $d = 4 - \epsilon$

We also solve the spectrum of single-trace bilinears in the theory in  $d = 4 - \epsilon$ , which allows us to determine analytic expressions for various quantities in terms of  $\lambda$ . In this section, it is convenient to absorb  $d_\gamma$  into the definition of  $\lambda$  by defining  $\hat{\lambda} = \frac{2M}{d_\gamma N}$ ; alternatively, one can set  $d_\gamma = 2$  and then  $\hat{\lambda} = \lambda$ .

### D.1 The gap equation

We first solve the gap equation. The allowed range for  $\Delta_\psi$  is  $\frac{3}{2} - \frac{\epsilon}{2} \leq \Delta_\psi \leq \frac{3}{2} - \frac{\epsilon}{4}$ . We find:

$$\Delta_\psi = \frac{3}{2} - \frac{(\hat{\lambda} + 2)\epsilon}{4(\hat{\lambda} + 1)} + \frac{\hat{\lambda}(5\hat{\lambda} - 6)\epsilon^2}{32(\hat{\lambda} + 1)^3} + O(\epsilon^3), \quad (\text{D.1})$$

and

$$\Delta_\sigma = 1 - \frac{\hat{\lambda}\epsilon}{2(\hat{\lambda} + 1)} - \frac{\hat{\lambda}(5\hat{\lambda} - 6)\epsilon^2}{16(\hat{\lambda} + 1)^3} + O(\epsilon^3). \quad (\text{D.2})$$

The critical value,  $\hat{\lambda}_*$ , of  $\hat{\lambda}$  at which  $2\Delta_\psi(\hat{\lambda}_*) - 1 = 2\Delta_\sigma(\hat{\lambda}_*)$  is given by  $\hat{\lambda}_* = 2 - \frac{\epsilon}{3} - \frac{\epsilon^2}{18} + O(\epsilon^3)$ .

### D.2 Parity-odd scalars

Solving for the spectrum of parity-odd scalars, we find the lowest scalar has scaling dimension given by:

$$\tilde{\Delta}_0 = 3 + \frac{(\hat{\lambda} - 2)\epsilon}{2(\hat{\lambda} + 1)} - \frac{\hat{\lambda}(14\hat{\lambda}^2 - 5\hat{\lambda} + 14)\epsilon^2}{16(\hat{\lambda} + 1)^3} + \frac{\hat{\lambda}(32\hat{\lambda}^4 - 57\hat{\lambda}^3 + 143\hat{\lambda}^2 - 153\hat{\lambda} - 22)\epsilon^3}{64(\hat{\lambda} + 1)^5} + O(\epsilon^4). \quad (\text{D.3})$$

The higher-twist parity odd scalars have dimension:

$$\begin{aligned} \tilde{\Delta}_n = & 2\Delta_\psi + 2n + \frac{8\epsilon^2\hat{\lambda}^2(\hat{\lambda} + 1)}{16(\hat{\lambda} + 1)^3n(n + 1)} \\ & + \frac{\epsilon^3\hat{\lambda}^2(4\hat{\lambda}(\hat{\lambda} + 1)(2n(n + 1)H_{n-1} + 1) + \hat{\lambda}^2(-7n^2 + n + 4) + \hat{\lambda}(n^2 + 13n + 4) - 2n(7n + 5))}{16(\hat{\lambda} + 1)^4n^2(n + 1)^2} + O(\epsilon^4) \end{aligned} \quad (\text{D.4})$$

The anomalous dimensions for large  $n$  are

$$\tilde{\gamma}_{0,n} \sim \frac{\hat{\lambda}^2}{2(\hat{\lambda} + 1)^2n^2}\epsilon^2 + \frac{\hat{\lambda}^2(\hat{\lambda}(-7\hat{\lambda} + 8\gamma(\hat{\lambda} + 1) + 1) + 8\hat{\lambda}(\hat{\lambda} + 1)\log n - 14)}{16(\hat{\lambda} + 1)^4n^2}\epsilon^3 + O(\epsilon^4), \quad (\text{D.5})$$

which is consistent with  $\tilde{\gamma}_{0,n} \sim \frac{1}{n^{2\Delta_\sigma}}$ .



### D.3 Parity-even scalars

We next compute the parity-even scalar spectrum. We find for the lowest twist parity-even scalars:

$$\Delta_0^A = 4 - \epsilon \quad (\text{D.6})$$

$$\begin{aligned} \Delta_0^B = 2 - & \frac{\left(\hat{\lambda} - \sqrt{\hat{\lambda}^2 + 14\hat{\lambda} + 1} + 1\right) \epsilon}{2\hat{\lambda} + 2} - \frac{\hat{\lambda} \left(35\hat{\lambda}^2 - 5\hat{\lambda} + 26\right) \epsilon^2}{8 \left((\hat{\lambda} + 1)^3 \sqrt{\hat{\lambda}^2 + 14\hat{\lambda} + 1}\right)} \\ & + \frac{3\hat{\lambda} \left(25\hat{\lambda}^6 + 136\hat{\lambda}^5 + 213\hat{\lambda}^4 + 3427\hat{\lambda}^3 + 336\hat{\lambda}^2 - 83\hat{\lambda} + 2\right) \epsilon^3}{32(\hat{\lambda} + 1)^5 \left(\hat{\lambda}^2 + 14\hat{\lambda} + 1\right)^{3/2}} + O(\epsilon^4) \end{aligned} \quad (\text{D.7})$$

The anomalous dimensions of type A higher twist parity-even scalars are,

$$\begin{aligned} \gamma_{0,n}^A = & \frac{\hat{\lambda}^2 \epsilon^2}{2(\hat{\lambda} + 1)^2 n(n + 2)} + \\ & \frac{\hat{\lambda}^2 \epsilon^3}{16(\hat{\lambda} - 2)(\hat{\lambda} + 1)^4 n^2 (n + 1)^2 (n + 2)^2} \left(8\hat{\lambda} (\hat{\lambda} - 2) (\hat{\lambda} + 1)(n + 1)^2 (n + 2)nH_{n-1} + 4 \left(3\hat{\lambda}^3 + \hat{\lambda}^2 + 6\hat{\lambda} + 8\right) \right. \\ & + \left(-7\hat{\lambda}^3 + 15\hat{\lambda}^2 - 16\hat{\lambda} + 28\right) n^4 - 4 \left(4\hat{\lambda}^3 - 13\hat{\lambda}^2 + 23\hat{\lambda} - 26\right) n^3 + \left(5\hat{\lambda}^3 + 43\hat{\lambda}^2 - 168\hat{\lambda} + 124\right) n^2 \\ & \left. + 2 \left(13\hat{\lambda}^3 - 3\hat{\lambda}^2 - 58\hat{\lambda} + 24\right) n\right) + O(\epsilon^4) \\ \sim_{n \rightarrow \infty} & \epsilon^2 \left(\frac{\hat{\lambda}^2}{2(\hat{\lambda} + 1)^2 n^2}\right) + \epsilon^3 \left(\frac{\hat{\lambda}^2 (\hat{\lambda} - 7\hat{\lambda}^2 + 8\hat{\lambda}(\hat{\lambda} + 1)(\log n + \gamma) - 14)}{16(\hat{\lambda} + 1)^4 n^2}\right) + O(\epsilon^4), \end{aligned} \quad (\text{D.8})$$

which is consistent with  $\gamma_{0,n}^A \sim n^{-2\Delta_\sigma}$  at large  $n$ . At finite  $n$ , the expression is slightly different when  $\hat{\lambda} = \hat{\lambda}_*$ .

For type B scalars, the  $n = 1$  operator needs to be handled separately:

$$\gamma_{0,1}^B = \frac{\hat{\lambda}}{\hat{\lambda} + 1} \epsilon - \frac{\hat{\lambda} \left(\hat{\lambda}^2 + 8\hat{\lambda} + 18\right)}{8(\hat{\lambda} + 1)^3} \epsilon^2 + O(\epsilon^3) \quad (\text{D.9})$$

For  $\hat{\lambda} \neq \hat{\lambda}_*$ , the type-B anomalous dimensions for  $n > 1$  are:

$$\gamma_{0,n}^B = -\frac{2\hat{\lambda} \left(\hat{\lambda} + 2\right)}{(\hat{\lambda} - 2)(\hat{\lambda} + 1)^3 n^2 (n^2 - 1)^2} \epsilon^3 + O(\epsilon^4), \quad (\text{D.10})$$

consistent with  $\gamma_{0,n}^B \sim n^{-4\Delta_\psi}$ .

For  $\hat{\lambda} = \hat{\lambda}_* = 2 - \epsilon/3 - \epsilon^2/18$  the type B anomalous dimensions for  $n > 1$  are:

$$\begin{aligned} \gamma_{0,n}^B(\hat{\lambda}_*) = & \frac{n - \sqrt{n^2 + 8}}{9n(n + 1)(n - 1)} \epsilon^2 + O(\epsilon^3) \\ \sim_{n \rightarrow \infty} & -\frac{4}{9n^4} \epsilon^2 - \frac{2(4 \log n + 4\gamma - 7)}{27n^4} \epsilon^3 + O(\epsilon^4), \end{aligned} \quad (\text{D.11})$$

consistent with  $\gamma_{0,n}^B(\hat{\lambda}_*) \sim n^{-(2\Delta_\psi + 1)}$ .

For type A scalars, at  $\hat{\lambda} = \hat{\lambda}_*$ , the anomalous dimensions at finite  $n$  also differ from the results at generic values of  $\hat{\lambda}$ :

$$\gamma^A(\hat{\lambda}_*)_{0,n} = \frac{n + \sqrt{(n + 1)^2 + 8} + 1}{9n(n + 2)(n + 3)} \epsilon + O(\epsilon)^2, \quad (\text{D.12})$$

but this does not affect the large  $n$  asymptotics.

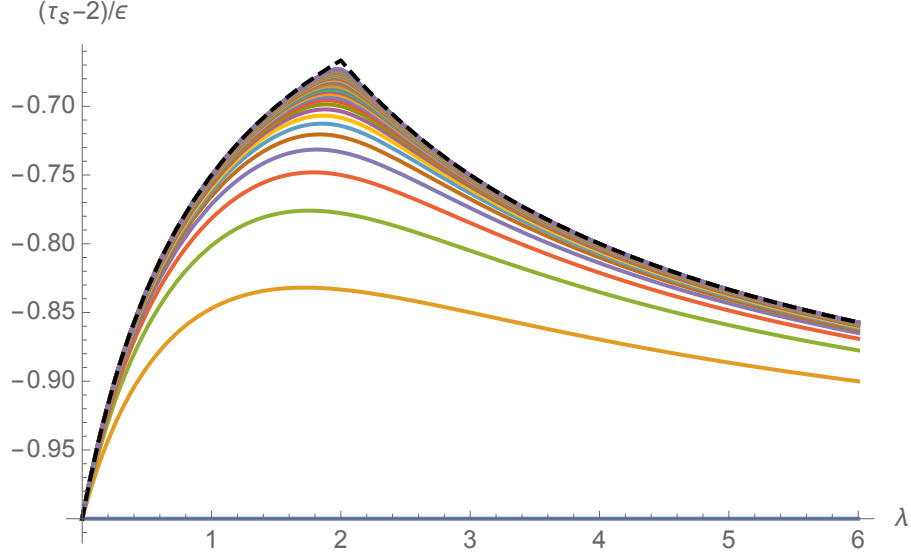


Figure 14: The  $O(\epsilon)$  contribution to the twist of leading-twist higher-spin operators in  $d = 4 - \epsilon$ , given in equation (D.14) is plotted for even spins  $2, 4, \dots, 100$ . The dashed line is the asymptotic behaviour as  $s \rightarrow \infty$ .

#### D.4 Leading twist higher-spin operators

Let us compute the leading twist higher-spin operators, which are parity-even.

For odd  $s$ , the leading-twist of a spin  $s$  operator with  $s \geq 1$ , is given by:

$$\begin{aligned}
\tau_{s,\min} &= 2\Delta_\psi - 1 - \frac{\hat{\lambda}}{(\hat{\lambda} + 1)(s^2 + s)}\epsilon + \\
&\frac{\hat{\lambda} \left( -4\hat{\lambda}(\hat{\lambda} + 1)((s + 1)^2 s^2 H_{s-1} + 1) + (7\hat{\lambda}^2 + 8\hat{\lambda} + 12)s^4 + 2(3\hat{\lambda}^2 + 8)s^3 - \hat{\lambda}(\hat{\lambda} + 12)s^2 - 4(\hat{\lambda} + 1)(2\hat{\lambda} + 1)s \right)}{8(\hat{\lambda} + 1)^3 s^3 (s + 1)^3} \epsilon^2 \\
&+ O(\epsilon^3) \\
&= 2 - \frac{\epsilon \left( \hat{\lambda} + \frac{2\hat{\lambda}}{s^2 + s} + 2 \right)}{2(\hat{\lambda} + 1)} + O(\epsilon^2).
\end{aligned} \tag{D.13}$$

For  $s$  even, the leading-twist of a spin  $s$  operator with  $s \geq 1$ , is given by:

$$\begin{aligned}
\tau_{s,\min} &= 2 - \frac{\epsilon \left( 2\hat{\lambda} + \sqrt{\hat{\lambda}^2 (s^2 + s - 2)^2 - 4\hat{\lambda}s(s^2 + s - 10)(s + 1) + 4s^2(s + 1)^2 + (3\hat{\lambda} + 2)s(s + 1)} \right)}{4(\hat{\lambda} + 1)s(s + 1)} \\
&+ O(\epsilon^2).
\end{aligned} \tag{D.14}$$

(We also computed the order  $\epsilon^2$  term for finite  $s$ , but we do not reproduce it here.) Equation (D.14) is plotted in Figure 14.

The large  $s$  behaviour of  $\tau_{s,\min}$  for  $s$  odd is

$$\begin{aligned}\gamma_s &= -\frac{\hat{\lambda}\epsilon}{(\hat{\lambda}+1)s^2} - \frac{\hat{\lambda}\epsilon^2 \left( (4\gamma - 7)\hat{\lambda}^2 + 4(\gamma - 2)\hat{\lambda} + 4(\hat{\lambda} + 1)\hat{\lambda} \log(s) - 12 \right)}{8(\hat{\lambda} + 1)^3 s^2} + O(\epsilon^3) \\ &= -\frac{\hat{\lambda}\epsilon}{(\hat{\lambda} + 1)s^2} - \frac{\epsilon^2 \hat{\lambda}^2 \log s}{2(\hat{\lambda} + 1)^2 s^2} + O(\epsilon^3)\end{aligned}\tag{D.15}$$

The smallest twist operator is the stress tensor, which has twist  $2 - \epsilon$ . However, all higher spin operators have twists  $2 + O(\epsilon)$ , and would also contribute to the term of order  $\epsilon^2 s^{-2} \log s$  in the above expression.

For operators with even spin, the large-spin behaviour of anomalous dimensions depends on whether or not  $\hat{\lambda}$  exceeds  $\hat{\lambda}_*$ . For  $\hat{\lambda} < 2 - \epsilon/3$ , the large spin anomalous dimensions, including  $\epsilon^2$  terms, are:

$$\gamma_s \sim -\frac{(\hat{\lambda} - 6)\hat{\lambda}\epsilon}{(\hat{\lambda} - 2)(\hat{\lambda} + 1)s^2} + \frac{\hat{\lambda}(\hat{\lambda}^2 - 6\hat{\lambda} - 8)}{2(\hat{\lambda} - 2)(\hat{\lambda} + 1)^2 s^2} \epsilon^2 \log s + O(\epsilon^3).\tag{D.16}$$

and, for  $\hat{\lambda} > 2 - \epsilon/3$ ,

$$\gamma_s \sim -\frac{4\hat{\lambda}\epsilon}{(\hat{\lambda} - 2)(\hat{\lambda} + 1)s^2} + \frac{2\hat{\lambda}(\hat{\lambda} + 2)}{(\hat{\lambda} - 2)(\hat{\lambda} + 1)^2 s^2} \epsilon^2 \log s + O(\epsilon^3).\tag{D.17}$$

Above, we only included terms of order  $\epsilon^n (\log s)^{n-1}$ . These expressions are consistent with the exchange of multiple operators with twists of order  $2 + O(\epsilon)$  in the four-point function.

The order  $\epsilon^2$  correction to  $\gamma_s$  for  $\hat{\lambda} = 2 - \epsilon/3$  is:

$$\begin{aligned}\gamma_s \Big|_{\hat{\lambda}=\hat{\lambda}_*} &= -\frac{2}{3s} \epsilon + \\ &\left( \frac{7s^4 + 8s^3 - 9s^2 - 9s - 2}{9s^3(s+1)(2s+1)} - \frac{2H_{s-1}}{9s} \right) \epsilon^2 + O(\epsilon^3) \\ &\rightarrow -\frac{2}{3s} \epsilon + \left( \frac{-4 \log(s) - 4\gamma + 7}{18s} \right) \epsilon^2 + O(\epsilon^3)\end{aligned}\tag{D.18}$$

This is consistent with

$$\gamma_s \sim \left( -\frac{2}{3} \epsilon \right) s^{-(1-\frac{\epsilon}{3})} = \left( -\frac{2}{3} \epsilon \right) s^{-\Delta_\sigma},\tag{D.19}$$

as would arise from exchange of the scalar field  $\sigma^a$ . It would be interesting to understand the large spin behaviour of the theory at  $\hat{\lambda}_*$  better via analytic bootstrap methods [96–101], assuming they can also be applied to the present disordered CFT, which appears to be unitary.<sup>9</sup>

## References

- [1] G. 't Hooft, “A Planar Diagram Theory for Strong Interactions,” *Nucl.Phys.* **B72** (1974) 461.
- [2] J. M. Maldacena, “The Large N limit of superconformal field theories and supergravity,” *Adv.Theor.Math.Phys.* **2** (1998) 231–252, [hep-th/9711200](#).
- [3] S. Gubser, I. R. Klebanov, and A. M. Polyakov, “Gauge theory correlators from noncritical string theory,” *Phys.Lett.* **B428** (1998) 105–114, [hep-th/9802109](#).

---

<sup>9</sup>We thank R. Sinha for raising this point.

- [4] E. Witten, “Anti-de Sitter space and holography,” *Adv.Theor.Math.Phys.* **2** (1998) 253–291, [hep-th/9802150](#).
- [5] G. 't Hooft, “A Two-Dimensional Model for Mesons,” *Nucl.Phys.* **B75** (1974) 461.
- [6] I. Klebanov and A. Polyakov, “AdS dual of the critical  $O(N)$  vector model,” *Phys.Lett.* **B550** (2002) 213–219, [hep-th/0210114](#).
- [7] E. Sezgin and P. Sundell, “Holography in 4D (super) higher spin theories and a test via cubic scalar couplings,” *JHEP* **0507** (2005) 044, [hep-th/0305040](#).
- [8] R. G. Leigh and A. C. Petkou, “Holography of the  $N=1$  higher spin theory on  $AdS(4)$ ,” *JHEP* **0306** (2003) 011, [hep-th/0304217](#).
- [9] S. Giombi, S. Minwalla, S. Prakash, S. P. Trivedi, S. R. Wadia, *et. al.*, “Chern-Simons Theory with Vector Fermion Matter,” *Eur.Phys.J.* **C72** (2012) 2112, [1110.4386](#).
- [10] O. Aharony, G. Gur-Ari, and R. Yacoby, “ $d=3$  Bosonic Vector Models Coupled to Chern-Simons Gauge Theories,” *JHEP* **1203** (2012) 037, [1110.4382](#).
- [11] J. Maldacena and A. Zhiboedov, “Constraining Conformal Field Theories with A Higher Spin Symmetry,” *J.Phys.* **A46** (2013) 214011, [1112.1016](#).
- [12] J. Maldacena and A. Zhiboedov, “Constraining conformal field theories with a slightly broken higher spin symmetry,” *Class.Quant.Grav.* **30** (2013) 104003, [1204.3882](#).
- [13] O. Aharony, O. Bergman, D. L. Jafferis, and J. Maldacena, “ $N=6$  superconformal Chern-Simons-matter theories, M2-branes and their gravity duals,” *JHEP* **10** (2008) 091, [0806.1218](#).
- [14] O. Aharony, O. Bergman, and D. L. Jafferis, “Fractional M2-branes,” *JHEP* **0811** (2008) 043, [0807.4924](#).
- [15] C.-M. Chang, S. Minwalla, T. Sharma, and X. Yin, “ABJ Triality: from Higher Spin Fields to Strings,” *J.Phys.* **A46** (2013) 214009, [1207.4485](#).
- [16] H. Ooguri and C. Vafa, “Non-supersymmetric AdS and the Swampland,” *Adv. Theor. Math. Phys.* **21** (2017) 1787–1801, [1610.01533](#).
- [17] S. Kapoor and S. Prakash, “Bifundamental Multiscalar Fixed Points in  $d = 3 - \epsilon$ ,” [2112.01055](#).
- [18] H. Osborn and A. Stergiou, “Seeking fixed points in multiple coupling scalar theories in the  $\epsilon$  expansion,” *JHEP* **05** (2018) 051, [1707.06165](#).
- [19] V. Gurucharan and S. Prakash, “Anomalous dimensions in non-supersymmetric bifundamental Chern-Simons theories,” *JHEP* **09** (2014) 009, [1404.7849](#). [Erratum: [JHEP11,045\(2017\)](#)].
- [20] V. Guru Charan and S. Prakash, “On the Higher Spin Spectrum of Chern-Simons Theory coupled to Fermions in the Large Flavour Limit,” *JHEP* **02** (2018) 094, [1711.11300](#).
- [21] R. Gurau, “Colored Group Field Theory,” *Commun. Math. Phys.* **304** (2011) 69–93, [0907.2582](#).
- [22] R. Gurau and V. Rivasseau, “The  $1/N$  expansion of colored tensor models in arbitrary dimension,” *Europhys. Lett.* **95** (2011) 50004, [1101.4182](#).
- [23] R. Gurau, “The complete  $1/N$  expansion of colored tensor models in arbitrary dimension,” *Annales Henri Poincare* **13** (2012) 399–423, [1102.5759](#).

- [24] V. Bonzom, R. Gurau, A. Riello, and V. Rivasseau, “Critical behavior of colored tensor models in the large  $N$  limit,” *Nucl. Phys.* **B853** (2011) 174–195, 1105.3122.
- [25] A. Tanasa, “Multi-orientable Group Field Theory,” *J. Phys.* **A45** (2012) 165401, 1109.0694.
- [26] V. Bonzom, R. Gurau, and V. Rivasseau, “Random tensor models in the large  $N$  limit: Uncoloring the colored tensor models,” *Phys. Rev.* **D85** (2012) 084037, 1202.3637.
- [27] S. Carrozza and A. Tanasa, “ $O(N)$  Random Tensor Models,” *Lett. Math. Phys.* **106** (2016), no. 11 1531–1559, 1512.06718.
- [28] E. Witten, “An SYK-Like Model Without Disorder,” *J. Phys. A* **52** (2019), no. 47 474002, 1610.09758.
- [29] I. R. Klebanov and G. Tarnopolsky, “Uncolored random tensors, melon diagrams, and the Sachdev-Ye-Kitaev models,” *Phys. Rev.* **D95** (2017), no. 4 046004, 1611.08915.
- [30] S. Prakash and R. Sinha, “Melonic Dominance in Subchromatic Sextic Tensor Models,” *Phys. Rev. D* **101** (2020), no. 12 126001, 1908.07178.
- [31] S. Sachdev and J. Ye, “Gapless spin fluid ground state in a random, quantum Heisenberg magnet,” *Phys. Rev. Lett.* **70** (1993) 3339, cond-mat/9212030.
- [32] A. Kitaev, “A simple model of quantum holography,” <http://online.kitp.ucsb.edu/online/entangled15/kitaev/>, <http://online.kitp.ucsb.edu/online/entangled15/kitaev2/> Talks at KITP, April 7 and May 27, 2015.
- [33] J. Maldacena and D. Stanford, “Remarks on the Sachdev-Ye-Kitaev model,” *Phys. Rev.* **D94** (2016), no. 10 106002, 1604.07818.
- [34] A. Kitaev and S. J. Suh, “The soft mode in the Sachdev-Ye-Kitaev model and its gravity dual,” *JHEP* **05** (2018) 183, 1711.08467.
- [35] V. Rosenhaus, “An introduction to the SYK model,” *J. Phys.* **A52** (2019), no. 32 323001.
- [36] W. Fu, D. Gaiotto, J. Maldacena, and S. Sachdev, “Supersymmetric Sachdev-Ye-Kitaev models,” *Phys. Rev. D* **95** (2017), no. 2 026009, 1610.08917. [Addendum: *Phys. Rev. D* **95**, 069904 (2017)].
- [37] A. Jevicki, K. Suzuki, and J. Yoon, “Bi-Local Holography in the SYK Model,” *JHEP* **07** (2016) 007, 1603.06246.
- [38] G. Mandal, P. Nayak, and S. R. Wadia, “Coadjoint orbit action of Virasoro group and two-dimensional quantum gravity dual to SYK/tensor models,” *JHEP* **11** (2017) 046, 1702.04266.
- [39] S. R. Das, A. Jevicki, and K. Suzuki, “Three Dimensional View of the SYK/AdS Duality,” *JHEP* **09** (2017) 017, 1704.07208.
- [40] S. R. Das, A. Ghosh, A. Jevicki, and K. Suzuki, “Three Dimensional View of Arbitrary  $q$  SYK models,” *JHEP* **02** (2018) 162, 1711.09839.
- [41] K. Bulycheva, I. R. Klebanov, A. Milekhin, and G. Tarnopolsky, “Spectra of Operators in Large  $N$  Tensor Models,” *Phys. Rev. D* **97** (2018), no. 2 026016, 1707.09347.
- [42] D. J. Gross and V. Rosenhaus, “The Bulk Dual of SYK: Cubic Couplings,” *JHEP* **05** (2017) 092, 1702.08016.
- [43] G. Turiaci and H. Verlinde, “Towards a 2d QFT Analog of the SYK Model,” *JHEP* **10** (2017) 167, 1701.00528.

- [44] J. Murugan, D. Stanford, and E. Witten, “More on Supersymmetric and 2d Analogs of the SYK Model,” *JHEP* **08** (2017) 146, 1706.05362.
- [45] J. Liu, E. Perlmutter, V. Rosenhaus, and D. Simmons-Duffin, “ $d$ -dimensional SYK, AdS Loops, and  $6j$  Symbols,” *JHEP* **03** (2019) 052, 1808.00612.
- [46] C.-M. Chang, S. Colin-Ellerin, C. Peng, and M. Rangamani, “A 3d disordered superconformal fixed point,” *JHEP* **11** (2021) 211, 2108.00027.
- [47] C.-M. Chang, S. Colin-Ellerin, C. Peng, and M. Rangamani, “Disordered Vector Models: From Higher Spins to Incipient Strings,” *Phys. Rev. Lett.* **129** (2022), no. 1 011603, 2112.09157.
- [48] S. Giombi, I. R. Klebanov, and G. Tarnopolsky, “Bosonic tensor models at large  $N$  and small  $\epsilon$ ,” *Phys. Rev. D* **96** (2017), no. 10 106014, 1707.03866.
- [49] S. Prakash and R. Sinha, “A Complex Fermionic Tensor Model in  $d$  Dimensions,” *JHEP* **02** (2018) 086, 1710.09357.
- [50] S. Giombi, I. R. Klebanov, F. Popov, S. Prakash, and G. Tarnopolsky, “Prismatic Large  $N$  Models for Bosonic Tensors,” *Phys. Rev.* **D98** (2018), no. 10 105005, 1808.04344.
- [51] J. Kim, E. Altman, and X. Cao, “Dirac Fast Scramblers,” *Phys. Rev. B* **103** (2021), no. 8 081113, 2010.10545.
- [52] D. J. Gross and A. Neveu, “Dynamical Symmetry Breaking in Asymptotically Free Field Theories,” *Phys. Rev.* **D10** (1974) 3235.
- [53] D. Benedetti, S. Carrozza, R. Gurau, and A. Sfondrini, “Tensorial Gross-Neveu models,” *JHEP* **01** (2018) 003, 1710.10253.
- [54] D. Benedetti, R. Gurau, and S. Harribey, “Line of fixed points in a bosonic tensor model,” *JHEP* **06** (2019) 053, 1903.03578.
- [55] A. Hasenfratz, P. Hasenfratz, K. Jansen, J. Kuti, and Y. Shen, “The Equivalence of the top quark condensate and the elementary Higgs field,” *Nuclear Physics* **365** (1991) 79–97.
- [56] J. Zinn-Justin, “Four-fermion interaction near four dimensions,” *Nuclear Physics B* **367** (1991), no. 1 105–122.
- [57] M. Moshe and J. Zinn-Justin, “Quantum field theory in the large  $N$  limit: A Review,” *Phys. Rept.* **385** (2003) 69–228, hep-th/0306133.
- [58] L. Fei, S. Giombi, I. R. Klebanov, and G. Tarnopolsky, “Yukawa CFTs and Emergent Supersymmetry,” *PTEP* **2016** (2016), no. 12 12C105, 1607.05316.
- [59] T. Muta and D. S. Popovic, “Anomalous Dimensions of Composite Operators in the Gross-Neveu Model in Two + Epsilon Dimensions,” *Prog. Theor. Phys.* **57** (1977) 1705.
- [60] W. Wetzel, “Two Loop Beta Function for the Gross-Neveu Model,” *Phys. Lett. B* **153** (1985) 297–299.
- [61] J. A. Gracey, “Calculation of exponent  $\eta$  to  $O(1/N^{**2})$  in the  $O(N)$  Gross-Neveu model,” *Int. J. Mod. Phys. A* **6** (1991) 395–408. [Erratum: *Int.J.Mod.Phys.A* 6, 2755 (1991)].
- [62] J. Zinn-Justin, “Four fermion interaction near four-dimensions,” *Nucl. Phys. B* **367** (1991) 105–122.
- [63] J. A. Gracey, “Computation of the three loop Beta function of the  $O(N)$  Gross-Neveu model in minimal subtraction,” *Nucl. Phys. B* **367** (1991) 657–674.

- [64] C. Luperini and P. Rossi, “Three loop Beta function(s) and effective potential in the Gross-Neveu model,” *Annals Phys.* **212** (1991) 371–401.
- [65] A. N. Vasiliev, S. E. Derkachov, N. A. Kivel, and A. S. Stepanenko, “The  $1/n$  expansion in the Gross-Neveu model: Conformal bootstrap calculation of the index  $\eta$  in order  $1/n^{**3}$ ,” *Theor. Math. Phys.* **94** (1993) 127–136.
- [66] J. A. Gracey, “Anomalous mass dimension at  $O(1/N^{**2})$  in the  $O(N)$  Gross-Neveu model,” *Phys. Lett. B* **297** (1992) 293–297.
- [67] N. A. Kivel, A. S. Stepanenko, and A. N. Vasiliev, “On calculation of  $(2+\epsilon)$  RG functions in the Gross-Neveu model from large  $N$  expansions of critical exponents,” *Nucl. Phys. B* **424** (1994) 619–627, [hep-th/9308073](#).
- [68] J. A. Gracey, “Computation of critical exponent  $\eta$  at  $O(1/N^{**3})$  in the four Fermi model in arbitrary dimensions,” *Int. J. Mod. Phys. A* **9** (1994) 727–744, [hep-th/9306107](#).
- [69] S. E. Derkachov, N. A. Kivel, A. S. Stepanenko, and A. N. Vasiliev, “On calculation in  $1/n$  expansions of critical exponents in the Gross-Neveu model with the conformal technique,” [hep-th/9302034](#).
- [70] J. A. Gracey, “Four loop  $\overline{MS}$  mass anomalous dimension in the Gross-Neveu model,” *Nucl. Phys. B* **802** (2008) 330–350, [0804.1241](#).
- [71] A. Raju, “ $\epsilon$ -Expansion in the Gross-Neveu CFT,” *JHEP* **10** (2016) 097, [1510.05287](#).
- [72] S. Ghosh, R. K. Gupta, K. Jaswin, and A. A. Nizami, “ $\epsilon$ -Expansion in the Gross-Neveu model from conformal field theory,” *JHEP* **03** (2016) 174, [1510.04887](#).
- [73] A. N. Manashov and E. D. Skvortsov, “Higher-spin currents in the Gross-Neveu model at  $1/n^2$ ,” *JHEP* **01** (2017) 132, [1610.06938](#).
- [74] J. A. Gracey, T. Luthe, and Y. Schroder, “Four loop renormalization of the Gross-Neveu model,” *Phys. Rev. D* **94** (2016), no. 12 125028, [1609.05071](#).
- [75] S. Giombi, V. Kirilin, and E. Skvortsov, “Notes on Spinning Operators in Fermionic CFT,” *JHEP* **05** (2017) 041, [1701.06997](#).
- [76] B. Kang and J. Yoon, “Sign-problem-free variant of the complex Sachdev-Ye-Kitaev model,” *Phys. Rev. B* **105** (2022), no. 4 045117, [2107.13572](#).
- [77] J. Kim, X. Cao, and E. Altman, “Low-rank Sachdev-Ye-Kitaev models,” *Phys. Rev. B* **101** (2020), no. 12 125112, [1910.10173](#).
- [78] Y. Wang, “Solvable Strong-coupling Quantum Dot Model with a Non-Fermi-liquid Pairing Transition,” *Phys. Rev. Lett.* **124** (2020), no. 1 017002, [1904.07240](#).
- [79] I. Esterlis and J. Schmalian, “Cooper pairing of incoherent electrons: an electron-phonon version of the Sachdev-Ye-Kitaev model,” *Phys. Rev. B* **100** (2019), no. 11 115132, [1906.04747](#).
- [80] E. Marcus and S. Vandoren, “A new class of SYK-like models with maximal chaos,” *JHEP* **01** (2019) 166, [1808.01190](#).
- [81] Z. Bi, C.-M. Jian, Y.-Z. You, K. A. Pawlak, and C. Xu, “Instability of the non-Fermi liquid state of the Sachdev-Ye-Kitaev Model,” *Phys. Rev. B* **95** (2017), no. 20 205105, [1701.07081](#).
- [82] A. A. Patel, H. Guo, I. Esterlis, and S. Sachdev, “Universal theory of strange metals from spatially random interactions,” [2203.04990](#).

- [83] H. Guo, I. Esterlis, A. A. Patel, and S. Sachdev, “Large  $N$  theory of critical Fermi surfaces II: conductivity,” 2207.08841.
- [84] V. Bonzom, V. Nador, and A. Tanasa, “Diagrammatic proof of the large  $N$  melonic dominance in the SYK model,” *Lett. Math. Phys.* **109** (2019), no. 12 2611–2624, 1808.10314.
- [85] S. Giombi, S. Prakash, and X. Yin, “A Note on CFT Correlators in Three Dimensions,” *JHEP* **1307** (2013) 105, 1104.4317.
- [86] S. Giombi and V. Kirilin, “Anomalous Dimensions in CFT with Weakly Broken Higher Spin Symmetry,” 1601.01310.
- [87] J. Polchinski and V. Rosenhaus, “The Spectrum in the Sachdev-Ye-Kitaev Model,” *JHEP* **04** (2016) 001, 1601.06768.
- [88] H. Osborn and A. Petkou, “Implications of conformal invariance in field theories for general dimensions,” *Annals Phys.* **231** (1994) 311–362, hep-th/9307010.
- [89] D. J. Gross and V. Rosenhaus, “A Generalization of Sachdev-Ye-Kitaev,” *JHEP* **02** (2017) 093, 1610.01569.
- [90] D. Chowdhury and E. Berg, “The unreasonable effectiveness of Eliashberg theory for pairing of non-Fermi liquids,” *Annals Phys.* **417** (2020) 168125, 1912.07646.
- [91] Y. Wang and A. V. Chubukov, “Quantum Phase Transition in the Yukawa-SYK Model,” *Phys. Rev. Res.* **2** (2020), no. 3 033084, 2005.07205.
- [92] I. Esterlis, H. Guo, A. A. Patel, and S. Sachdev, “Large  $N$  theory of critical Fermi surfaces,” *Phys. Rev. B* **103** (2021), no. 23 235129, 2103.08615.
- [93] J. Kim, I. R. Klebanov, G. Tarnopolsky, and W. Zhao, “Symmetry Breaking in Coupled SYK or Tensor Models,” *Phys. Rev. X* **9** (2019), no. 2 021043, 1902.02287.
- [94] I. R. Klebanov, A. Milekhin, G. Tarnopolsky, and W. Zhao, “Spontaneous Breaking of  $U(1)$  Symmetry in Coupled Complex SYK Models,” *JHEP* **11** (2020) 162, 2006.07317.
- [95] Y. Zhao, “Large- $N$  SYK Models,” Master’s thesis, (Bachelor’s Thesis) Princeton University, 2021.
- [96] L. F. Alday and J. M. Maldacena, “Comments on operators with large spin,” *JHEP* **11** (2007) 019, 0708.0672.
- [97] Z. Komargodski and A. Zhiboedov, “Convexity and Liberation at Large Spin,” *JHEP* **11** (2013) 140, 1212.4103.
- [98] A. L. Fitzpatrick, J. Kaplan, D. Poland, and D. Simmons-Duffin, “The Analytic Bootstrap and AdS Superhorizon Locality,” *JHEP* **12** (2013) 004, 1212.3616.
- [99] R. Gopakumar, A. Kaviraj, K. Sen, and A. Sinha, “Conformal Bootstrap in Mellin Space,” *Phys. Rev. Lett.* **118** (2017), no. 8 081601, 1609.00572.
- [100] P. Dey, A. Kaviraj, and A. Sinha, “Mellin space bootstrap for global symmetry,” *JHEP* **07** (2017) 019, 1612.05032.
- [101] A. Bissi, A. Sinha, and X. Zhou, “Selected Topics in Analytic Conformal Bootstrap: A Guided Journey,” 2202.08475.